

## VIP Very Important Paper

Benzofuroxan Derivatives as Potent Agents against Multidrug-Resistant *Mycobacterium tuberculosis*

Guilherme F. S. Fernandes<sup>+, [a, b]</sup> Débora L. Campos<sup>+, [a]</sup> Isabel C. Da Silva,<sup>[a]</sup>  
João L. B. Prates,<sup>[a, b]</sup> Aline R. Pavan,<sup>[a, b]</sup> Fernando R. Pavan,<sup>\*, [a]</sup> and Jean L. Dos Santos<sup>\*, [a, b]</sup>

Tuberculosis (TB) is currently the leading cause of death related to infectious diseases worldwide, as reported by the World Health Organization. Moreover, the increasing number of multidrug-resistant tuberculosis (MDR-TB) cases has alarmed health agencies, warranting extensive efforts to discover novel drugs that are effective and also safe. In this study, 23 new compounds were synthesized and evaluated *in vitro* against the drug-resistant strains of *M. tuberculosis*. The compound 6-((3-

fluoro-4-thiomorpholinophenyl)carbamoyl)benzo[c][1,2,5]oxadiazole 1-*N*-oxide (**5b**) was particularly remarkable in this regard as it demonstrated MIC<sub>90</sub> values below 0.28  $\mu$ M against all the MDR strains evaluated, thus suggesting that this compound might have a different mechanism of action. Benzofuroxans are an attractive new class of anti-TB agents, exemplified by compound **5b**, with excellent potency against the replicating and drug-resistant strains of *M. tuberculosis*.

## Introduction

Tuberculosis (TB) is one of the deadliest diseases affecting humankind. Historical evidence suggests that the common ancestor of all the modern members of the *Mycobacterium tuberculosis* (*M.tb*) family might have first appeared around 35 000–15 000 years ago.<sup>[1,2]</sup> *M.tb* is the main causative agent of tuberculosis in humans. According to the World Health Organization (WHO), TB was the leading cause of deaths due to infectious diseases in 2019, among which 1.4 million deaths occurred in HIV-negative people and 251 000 deaths occurred in HIV-positive people. This scenario is alarming, as in 2019, around 10 million new cases of TB were reported.<sup>[3]</sup>

Even though the number of confirmed deaths due to TB has been decreasing in recent years,<sup>[4–6]</sup> the scientific community and the health agencies around the world are particularly concerned regarding the high and rising numbers of multidrug-resistant tuberculosis [MDR-TB; defined as resistant to at least rifampicin (RIF) and isoniazid (INH)] and extensively drug-resistant tuberculosis [XDR-TB; defined as MDR plus an additional resistance to at least one fluoroquinolone and one

second-line injectable drug] strains.<sup>[7,8]</sup> According to the WHO's latest report, there were an estimated 465 000 incident cases of MDR-TB and 214 000 deaths due to MDR-TB in 2019. The cases were mainly concentrated in three countries: India (27%), China (14%), and the Russian Federation (8%).<sup>[3]</sup> The emergence of totally drug-resistant TB strains (TDR-TB)<sup>[9,10]</sup> has worsened the general scenario concerning the TB disease. TDR-TB refers to those *M.tb* clinical strains that exhibit *in vitro* resistance to all first- and second-line drugs tested.<sup>[11]</sup> This situation of TDR-TB is critical, as there is a lack of drugs that can be used against the MDR strains. Although the WHO does not use the term TDR-TB specifically, such cases continue to appear<sup>[12]</sup> across the world, mainly in Africa, Eastern Europe, China, and India.<sup>[13–15]</sup>

In view of the worrying number of cases of this disease, the WHO finally stated that “without novel anti-*M.tb* drugs and regimens, it would be quite difficult to improve treatment outcomes of this disease in the near future”; this highlights the important role of the research and development aimed at identifying novel drugs to fight against this disease.<sup>[4]</sup> The current therapeutic regimen recommended by the WHO for the treatment of TB involves the use of a series of drugs classified as the first- and second-line treatment. The first-line drugs include INH, RIF, ethambutol (EMB), and pyrazinamide (PZA), and the second-line drugs include fluoroquinolones, aminoglycosides, D-cycloserine (DCS), linezolid (LZD), and bedaquiline (BDQ), among others.<sup>[7,16,17]</sup> However, a considerable number of these drugs were developed several years ago and, therefore, present certain limitations, such as prolonged standard regimen, high rate of treatment discontinuation, adverse effects, toxicity, drug–drug interactions, and lack of effectiveness against the most-resistant strains of *Mycobacteria*.<sup>[18–23]</sup>

Although the investment in the research and development of novel drugs against TB is far from the \$2 billion a year recommended as necessary by “The End TB Strategy” to eliminate the disease by 2030,<sup>[24]</sup> important advances have been achieved in recent years. After a period of over 50 years in which no novel drugs were approved for TB, three novel drugs

[a] Dr. G. F. S. Fernandes,<sup>+</sup> Dr. D. L. Campos,<sup>+</sup> Dr. I. C. Da Silva,  
Dr. J. L. B. Prates, Prof. A. R. Pavan, Prof. F. R. Pavan, Prof. J. L. Dos Santos  
School of Pharmaceutical Sciences  
São Paulo State University (UNESP)  
Araraquara Jaú Highway KM 01, 14800903 Araraquara (Brazil)  
E-mail: jean.santos@unesp.br  
fernando.pavan@unesp.br  
guilhermefelipe@outlook.com

[b] Dr. G. F. S. Fernandes,<sup>+</sup> Dr. J. L. B. Prates, Prof. A. R. Pavan,  
Prof. J. L. Dos Santos  
Institute of Chemistry  
São Paulo State University (UNESP)  
Francisco Degni Street 55, 14800060 Araraquara (Brazil)

[<sup>+</sup>] These authors contributed equally to this work.



Supporting information for this article is available on the WWW under  
<https://doi.org/10.1002/cmdc.202000899>



This article belongs to the Special Collection “BrazMedChem 2019: Medicinal Chemistry in Latin America”.

have recently been approved by the regulatory agencies (Figure 1). One of these drugs is bedaquiline (Sirturo<sup>®</sup>; Janssen Therapeutics), which was first approved in 2012 by the U.S. Food and Drug Administration (FDA) for the treatment of MDR-TB. The mechanism of action of bedaquiline involves the energy metabolism of replicating and nonreplicating mycobacteria.<sup>[25]</sup> The other two approved drugs, delamanid and pretomanid, are representatives of the nitroimidazole class. Delamanid (Deltysba<sup>®</sup>; Otsuka Pharmaceutical) was first approved in 2014 by the European Medicines Agency (EMA) and the Japanese regulatory authority, while pretomanid (TB Alliance) was approved by the FDA in 2019 for use in combination with BDQ and LZD for the treatment of highly drug-resistant forms of pulmonary TB (XDR-TB or treatment-intolerant/non-responsive MDR-TB).<sup>[26]</sup> Both these nitroimidazoles act by inhibiting the biosynthesis of mycolic acids.<sup>[27,28]</sup>

Several other drug candidates are currently in clinical phase studies, such as SQ109, delpazolid (LCB01-0371), sutezolid, telacebec (Q203), macozinone (PBTZ169), GSK-3036656, etc.<sup>[29]</sup> In this context and considering The End TB Strategy to eradicate TB, continual research and development of novel anti-TB compounds are crucial. We, as well as other researchers, have previously reported a series of benzofuroxan (Bfx) derivatives with potent activity against *M.tb*, including the MDR strains.<sup>[30,31]</sup> Our first study demonstrated the potential of these compounds as antimycobacterial agents by assessing their activity and cytotoxicity profile,<sup>[30]</sup> while the subsequent studies evaluated the *in vivo* efficacy and the mode of action of these compounds.<sup>[31]</sup> In particular, the compound (*E*)-6-((2-isonicotinoylhydrazono)methyl)benzo[*c*][1,2,5]oxadiazole 1-*N*-oxide (BZ8; Figure 1) could reduce the burden of *M.tb* to undetectable levels in a mouse model of TB infection.<sup>[31]</sup> Moreover, BZ8 was also active against several *M.tb* mono-resistant strains, including those with resistance to INH, RIF, BDQ, moxifloxacin (MOX), capreomycin (CAP), and streptomycin (SM). The MIC<sub>90</sub> values of BZ8 against these strains ranged from 1.2 to 16.9  $\mu$ M. Further studies revealed that BZ8 exhibited high intracellular inhibition (ca. 90%) and an early bactericidal effect.<sup>[31]</sup> However, the compound has low stability in the acid medium due to the presence of the *N*-acylhydrazone subunit and a poor anti-*M.tb* activity against the MDR strains (MIC<sub>90</sub> > 25  $\mu$ M). Therefore, despite the excellent *in vivo* activity demonstrated by BZ8, we

decided to continue the drug development process to find ways to overcome the chemical instability and improving the potency of the compound against the MDR-*M.tb* strains. Therefore, in an attempt to identify novel anti-*M.tb* compounds based on BZ8 optimization, the present study reports the synthesis and anti-*M.tb* activity of novel Bfx derivatives designed to serve as better alternatives for the treatment of MDR-TB.

## Results and Discussion

### Drug design

The initial phase of the BZ8 optimization strategy involved replacing the *N*-acylhydrazone subunit of this compound with an amide bond (Figure 2) to increase the chemical stability of the generated series of compounds, as certain *N*-acylhydrazone subunits exhibit chemical instability at acidic pH. The experimental results indicated that the derivatives containing the *N*-acylhydrazone subunit were poorly stable or completely unstable at acidic pH. This finding was consistent with the previous works published by our research group.<sup>[31–33]</sup> Therefore, the substitution of the *N*-acylhydrazone subunit was performed to overcome this inherent chemical instability. Similar to the *N*-acylhydrazone subunit-containing drug, the amide-containing drugs are also susceptible to hydrolysis, although at a much slower rate.

In the next step, the pyridine ring present in BZ8 was replaced with the fluorine-substituted phenyl ring attached to a morpholine ring at the *para* position relative to the amide bond. The efficiency of the synthesized compound **5c** was evaluated against several MDR-*M.tb* strains. The initial evaluation of the newly synthesized compound **5c** was performed against MDR strains rather than H<sub>37</sub>Rv because the objective of this initial stage of drug design was to assess whether changes in BZ8 would increase the potential of the compound against resistant strains. Indeed, the novel synthesized compound presented better results against these MDR strains compared to BZ8, with the MIC<sub>90</sub> values ranging between 1.81 and 5.23  $\mu$ M. This promising result against the resistant strains was sufficient motivation to expand the series of compounds by evaluating the different substituents attached to the fluorine-substituted

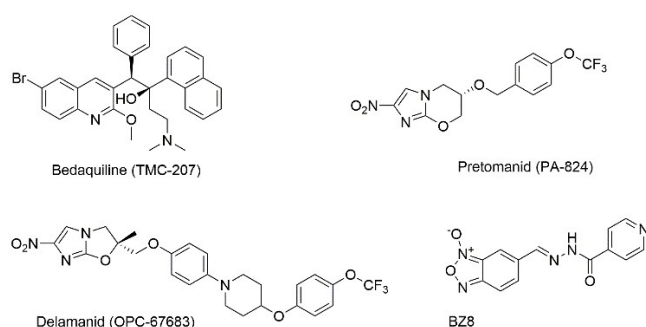


**Figure 1.** Recently approved drugs for the MDR-TB treatment and the lead benzofuroxan BZ8.

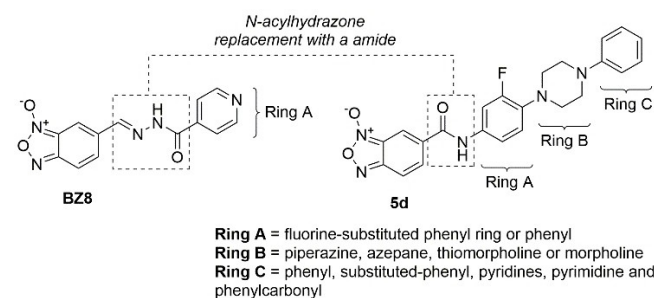


**Figure 2.** Example of the expansion of the chain of rings linked to the benzofuroxan nucleus. In the figure, compound **5d** is used as a model to exemplify the three-ring systems.

phenyl ring, including the cyclic amines and the substituted piperazines with different aromatic/heteroaromatic rings. Therefore, further experiments were focused on expanding the substituting chain of the rings attached to the Bfx nucleus. First, the 4-pyridine ring (ring A) present in BZ8 was replaced with a fluorine-substituted phenyl ring (ring A) and a cyclic amine (ring B) in the *para* position relative to the amide bond (Figure 2).

The structures of compounds **5a–5c** contain different cyclic amines attached to the fluorine-substituted central phenyl ring, including 1-azepanyl (compound **5a**), 4-thiomorpholiny (compound **5b**), and 4-morpholiny (compound **5c**), while the other compounds contain a piperazine ring (ring B) attached to the fluorine-substituted phenyl ring (ring A; compounds **5d–5q**). Furthermore, these compounds contain other aromatic/heteroaromatic rings (ring C) attached at the *para* position of the piperazine ring (Figure 2). Different rings, including phenyl, substituted-phenyl, pyridines, pyrimidine, and phenylcarbonyl rings, were selected.

The aim was to evaluate the actual contribution of the terminal part of the molecule to the anti-*M.tb* activity. Subsequently, the most active compound obtained in the first series was selected, and in its structure, the Bfx subunit was exchanged with other heterocycles. Several heterocycles, including benzofurazan **11a**, indole **11b**, benzimidazole **11c**, tetrazole **11d**, and 2-nitroaniline **11e**, were evaluated. In addition, the fluorine atom was replaced with a hydrogen atom in the most active compound obtained in the previous series. These changes in the most active compound produced the second series of compounds. The aim was to explore the influence of the Bfx subunit and the fluorine atom on the biological activity of the final compounds (Figure 3).

The Bfx derivatives represent an important scaffold in medicinal chemistry owing to their wide spectrum of biological activities,<sup>[34,35]</sup> including the anti-*M.tb* activity.<sup>[30,31]</sup> The antimycobacterial activity of these compounds is attributed to the reactive oxygen species (ROS) formed after their biotransformation.<sup>[36][37,38]</sup> The presence of the =N(→O)O– subunit in the Bfx scaffold might confer electron-accepting properties similar to those in the nitroaromatic compounds or *N*-oxides, which are

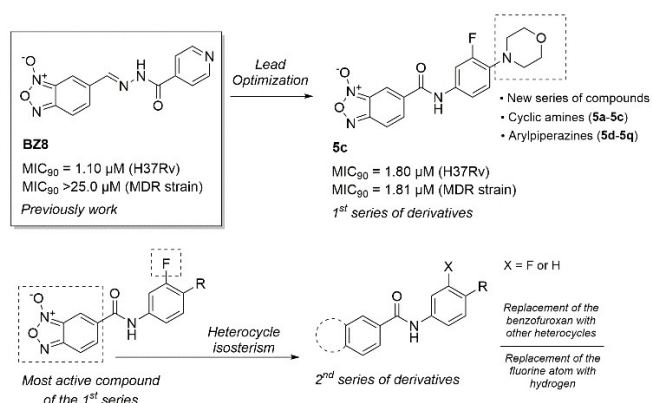


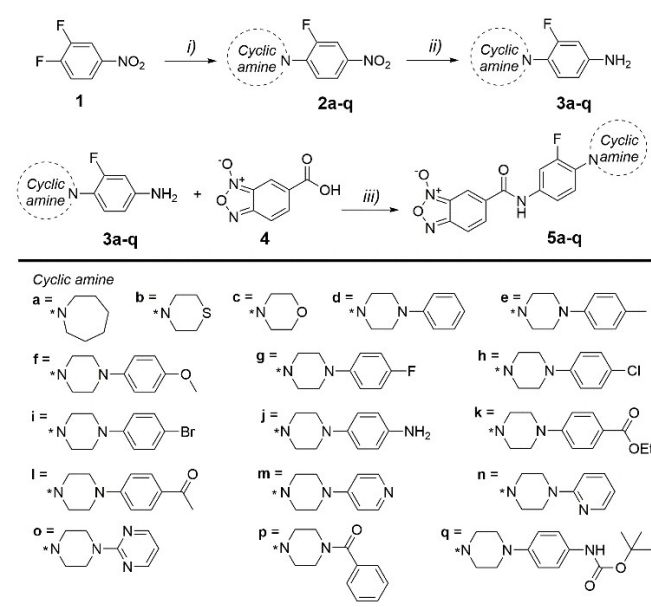
Figure 3. Design of the new series of benzofuroxan derivatives.

used widely as anti-cancer and cytotoxic agents activated after bioreduction.<sup>[39]</sup> ROS play a crucial role in the pathogenesis of TB. For instance, enhanced levels of ROS may damage the cellular components, such as lipids, proteins, and nucleic acids, thereby inhibiting *M.tb* growth.<sup>[40–43]</sup> Moreover, the Bfx derivatives may interact with the thiol (–SH) groups present in cysteine residues, which is considered a parallel mechanism of action underlying Bfx cytotoxicity.<sup>[44–46]</sup>

## Chemistry

First, a series of nitroaromatics *para*-substituted with cyclic amines, **2a–2q**, were synthesized. The nitroaromatic intermediates **2a–2q** were obtained by exploring the nucleophilic aromatic substitution reactions between 3,4-difluoronitrobenzene **1** and the appropriate cyclic amine. This reaction was performed using anhydrous acetonitrile heating at reflux and *N,N*-diisopropylethylamine (DIPEA) as the non-nucleophilic base (Scheme 1). The nitroaromatic intermediates were obtained in good yields (60–99%). The next step was the reduction of the aromatic nitro group into amine group, and the reaction was performed using ammonium chloride (NH<sub>4</sub>Cl) and iron powder as reducing agents in a mixture of ethanol/H<sub>2</sub>O, followed by heating at 90 °C (Scheme 1). This reduction reaction produced the aniline intermediates **3a–3q** in moderate yields (13–79%). The synthetic intermediates **2a–2q** and **3a–3q** were synthesized following the procedures reported previously.<sup>[47–49]</sup> The chemical characterization data of all the synthetic intermediates are provided in the Supporting Information.

The final step was to obtain the first series of compounds by coupling the Bfx derivative **4** with the aniline derivatives **2a–**



Scheme 1. Synthesis of the first series of compounds. i) The corresponding amine, DIPEA, acetonitrile, reflux, 6 h; ii) NH<sub>4</sub>Cl, Fe, ethanol/H<sub>2</sub>O, 90 °C, 1 h; iii) CDI, acetonitrile, 24 h.

**2q** for the formation of amide. Bfx **4** was obtained using the methodology described previously.<sup>[50]</sup> The reaction was performed in anhydrous acetonitrile in the presence of carbon-diimidazole (CDI) as the coupling agent, producing the final compounds of the 1<sup>st</sup> series, **5a–5q**, in moderate yields (10–97%; Scheme 1). The <sup>1</sup>H and <sup>13</sup>C nuclear magnetic resonance (NMR) spectra of these final compounds contained broad peaks corresponding to the proton and carbon signals from the Bfx subunit, indicating Bfx tautomerism.<sup>[34,38]</sup>

The synthesis of the second series of compounds was performed by following the same methodologies as for the first series of compounds. First, the aniline derivative **3n** was synthesized, which was then treated with different heterocycles using CDI as the coupling agent for amide bond formation, thereby producing the final compounds of the second series, **11a–11f**, in moderate yields (20–71%; Scheme 2). The carboxylic acid indole **7**, benzimidazole **8**, and 2-nitroaniline **10** intermediates were purchased commercially. The Bfx **6** and tetrazole **9** intermediates were synthesized using the methodologies reported previously.<sup>[51,52]</sup> The final compound of the second series, **11f** was obtained in a manner similar to the synthesis of compound **5n** of the first series. However, an aniline derivative containing a hydrogen atom, **13**, was used in place of the parent compound containing the fluorine atom, **3n**. The synthetic intermediates **3n** and **12** were synthesized by following previously described procedures.<sup>[47–49]</sup>

### Initial *in vitro* biological studies

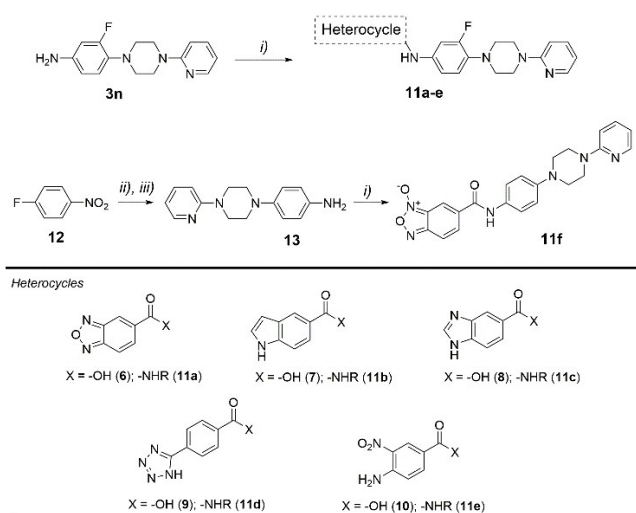
Initially, all the first series compounds were evaluated against the sensitive strains of *M.tb* H<sub>37</sub>Rv ATCC 27294 using the resazurin microtiter assay (REMA) methodology.<sup>[32,53,54]</sup> The results were expressed as the minimum inhibitory concentration (MIC<sub>90</sub>). The final compounds of the first series exhibited

potent antimycobacterial activity against *M.tb*, with MIC<sub>90</sub> values ranging from 0.09 to 31.60 μM (Table 1).

Determining the structure-activity relationship (SAR) for this series was challenging as neither steric nor electronic effects appeared to present any clear dominant trend. Nonetheless, certain patterns were observed and are discussed ahead. A SAR analysis of the first series of compounds revealed that this novel class of anti-*M.tb* compounds support, to a certain extent, structural variations in the portion of the molecule linked to the cyclic amine, as inferred from the retaining of the anti-*M.tb* activity after the exchange of substituents or the bioisosteric replacement of similar rings. This relationship could be clearly observed in the series containing halogens linked at the *para* position of the terminal phenyl ring. The compounds containing fluorine (**5g**), chlorine (**5h**), and bromine (**5i**) atoms attached at the *para* position exhibited MIC<sub>90</sub> values of 3.82, 2.69, and 2.53 μM, respectively. A similar relationship could be observed for compounds **5e** and **5f**, which contained methyl and methoxy groups, respectively, linked at the *para* position of the phenyl ring, with the compounds exhibiting MIC<sub>90</sub> values of 7.96 and 6.98 μM, respectively. Nevertheless, when an amine group was inserted in this position (compound **5j**), the MIC<sub>90</sub> value of 1.84 μM was achieved, thus indicating that the groups acting as hydrogen bond donors are important for the biological activity. Regarding the large substituents, it was not possible to observe a direct SAR as the compounds **5k** and **5q** that contained large groups exhibited varied MIC<sub>90</sub> values. Compound **5k** exhibited an MIC<sub>90</sub> value of 10.97 μM, while compound **5q** exhibited an MIC<sub>90</sub> value of 0.78 μM. A possible explanation for this variation could be the presence of a nitrogen donor for hydrogen bonding in compound **5q**.

The isosteric replacement of the phenyl ring attached to the piperazine with different heteroaromatic rings led to similar effects on the anti-*M.tb* activity. The exchange of the phenyl ring in compound **5d** with a pyridine ring in compound **5m** led to a loss in the antimycobacterial activity. However, when the nitrogen in the pyridine ring was added to a different position in the ring (compound **5n**), the anti-*M.tb* activity was increased significantly. Compound **5n** was the most active in this series, exhibiting an MIC<sub>90</sub> value of 0.09 μM. Similarly, compound **5o** containing a pyrimidine ring attached to the piperazine exhibited a MIC value of 2.22 μM.

Furthermore, the piperazinyl moiety was replaced with other isosteric rings, such as 1-azepanyl (compound **5a**), 4-thiomorpholinyl (compound **5b**), and 4-morpholinyl (compound **5c**). The compound containing the 4-thiomorpholinyl ring (**5b**) demonstrated promising anti-*M.tb* activity with an MIC<sub>90</sub> value of 0.70 μM. On the other hand, its bioisostere containing a morpholine ring (**5c**) exhibited an MIC<sub>90</sub> value of 5.22 μM, thus indicating that the bioisosteric replacement of oxygen atom with sulfur in the cyclic amine leads to a significant increase in the biological activity. The 1-azepanyl derivative (**5a**) exhibited an MIC<sub>90</sub> value of 2.89 μM. An attempt to establish a structure-activity relationship between these compounds by considering their lipophilicity was not successful.



**Scheme 2.** Synthesis of the second series of compounds. i) The corresponding carboxylic acid, CDI, acetonitrile, 24 h; ii) 1-(2-pyridyl)piperazine, DIPEA, acetonitrile, reflux, 6 h; iii) NH<sub>4</sub>Cl, Fe, ethanol/H<sub>2</sub>O, 90 °C, 1 h.

**Table 1.** Anti-M.tb activity of the first series against M.tb H<sub>37</sub>Rv (MIC<sub>90</sub>), cytotoxicity against the MRC-5 cell line (IC<sub>50</sub>), selectivity index (SI), clog*D*, and LiPE.

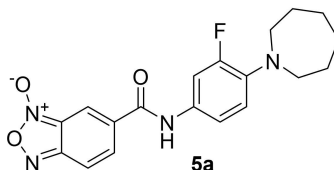
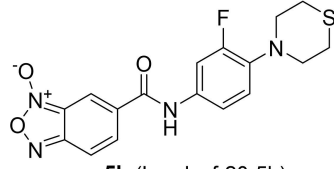
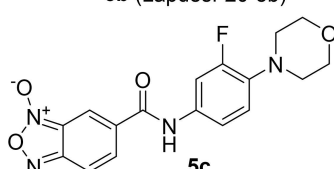
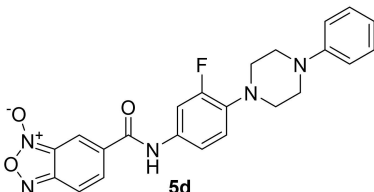
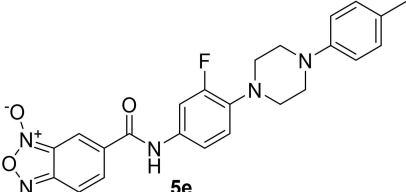
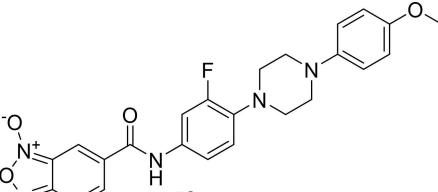
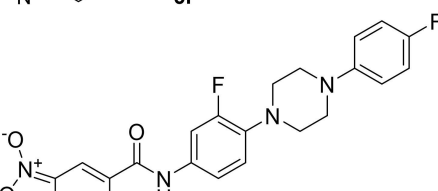
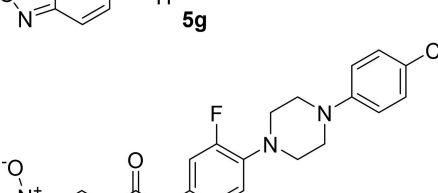
Compound	MIC <sub>90</sub> [μM]	IC <sub>50</sub> [μM]	SI	clog <i>D</i>	LiPE
 <b>5a</b>	2.89 ± 1.55	174.47	60	2.83	2.71
 <b>5b</b> (Lapdesf-20-5b)	0.70 ± 0.26	57.07	81	1.95	4.20
 <b>5c</b>	5.22 ± 2.33	58	11	1.37	3.91
 <b>5d</b>	11.75 ± 3.19	> 230	> 19	3.66	1.27
 <b>5e</b>	7.96 ± 4.07	> 223.48	> 28	4.11	1.06
 <b>5f</b>	6.98 ± 3.81	> 215.76	> 30	3.81	1.36
 <b>5g</b>	3.82 ± 1.36	> 221.52	> 58	3.70	1.72
 <b>5h</b>	2.69 ± 1.12	> 213.73	> 79	4.22	0.96



Table 1. continued

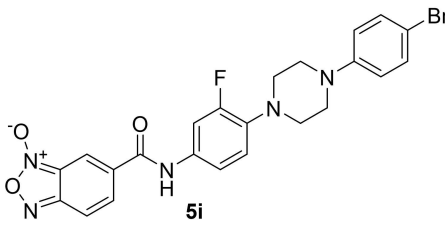
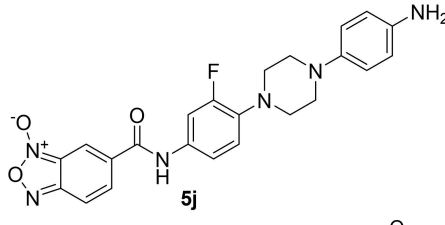
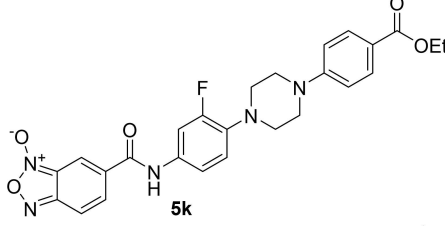
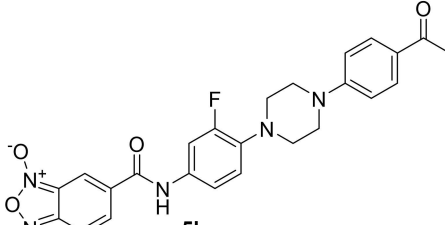
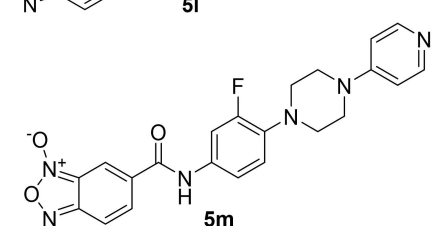
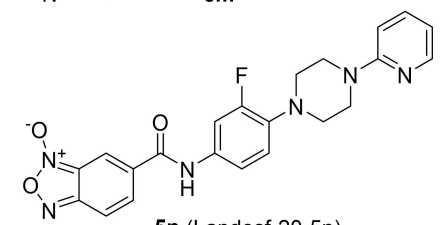
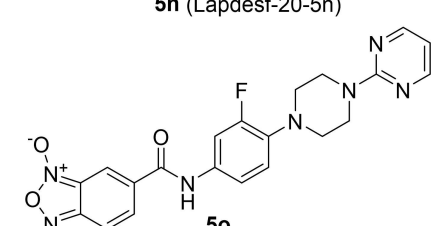
Compound	MIC <sub>90</sub> [μM]	IC <sub>50</sub> [μM]	SI	clog <i>D</i>	LiPE
 <b>5i</b>	2.53 ± 1.29	> 195.18	> 77	4.46	1.07
 <b>5j</b>	1.84 ± 0.94	> 223.11	> 121	2.68	3.03
 <b>5k</b>	10.97 ± 3.60	> 197.82	> 18	4.62	0.34
 <b>5l</b>	1.56 ± 0.85	> 210.31	> 134	3.01	2.16
 <b>5m</b>	18.19 ± 9.26	127.81	7	1.37	3.37
 <b>5n</b> (Lapdesf-20-5n)	0.09 ± 0.04	> 180.04	> 2085	2.80	4.25
 <b>5o</b>	2.22 ± 1.20	> 229.66	> 103	2.21	3.28

Table 1. continued

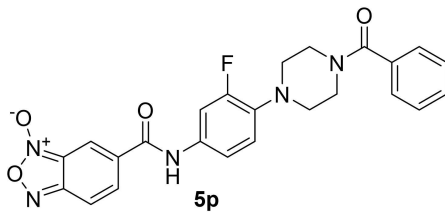
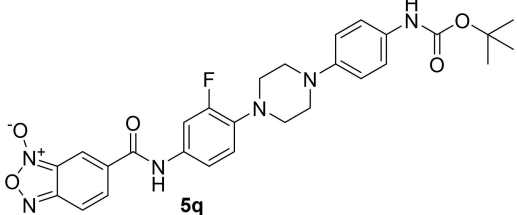
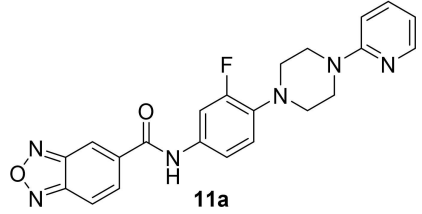
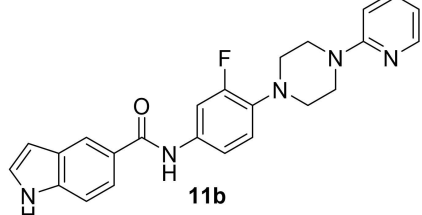
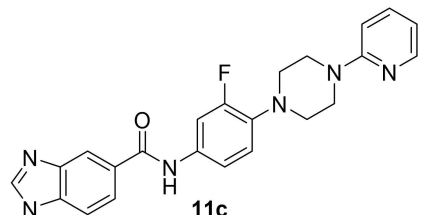
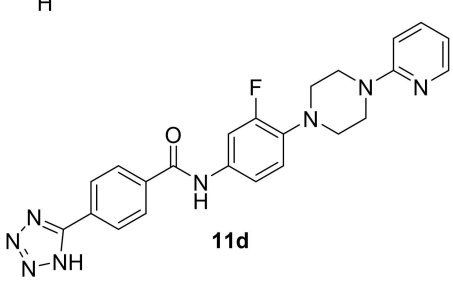
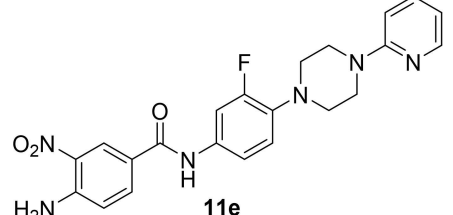
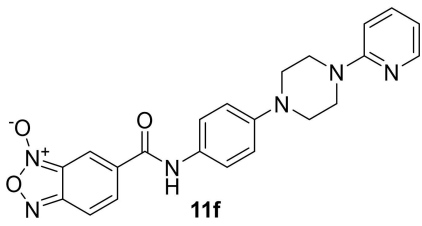
Compound	MIC <sub>90</sub> [μM]	IC <sub>50</sub> [μM]	SI	clogD	LiPE
 <b>5p</b>	2.45 ± 1.01	28.14	11	2.54	3.06
 <b>5q</b>	0.78 ± 0.40	> 182.28	> 233	4.48	1.32
 <b>11a</b>	> 25	N.D.	N.D.	3.68	N.D.
 <b>11b</b>	> 25	N.D.	N.D.	4.43	N.D.
 <b>11c</b>	> 25	N.D.	N.D.	3.62	N.D.
 <b>11d</b>	> 25	N.D.	N.D.	2.03	N.D.
 <b>11e</b>	> 25	N.D.	N.D.	4.09	N.D.

Table 1. continued

Compound	MIC <sub>90</sub> [μM]	IC <sub>50</sub> [μM]	SI	clogD	LiPE
 11f	2.5 ± 1.08	> 240.13	> 96	2.81	2.79
INH	0.95 ± 0.43	> 729.18	> 1695	−0.69	6.71
RIF	0.05 ± 0.01	> 121.51	> 2430	2.06	5.24
LZD	0.74 ± 0.29	N.D.	N.D.	0.64	5.49
BZ8	1.10	519.20	472	0.13	5.83

INH: isoniazid; RIF: rifampicin; LZD: linezolid; N.D.: not determined; cLog D: calculated distribution coefficient; LiPE: lipophilic efficiency; ±: standard deviation (SD), average of three independent assays.

Compound **5p** exhibited an MIC<sub>90</sub> value of 2.45 μM. This compound is a retroisostere of compound **5l** and contains a phenylcarbonyl group attached in reverse to the piperazine ring. This retroisosterism produced a significant increase in the anti-*M.tb* activity of compound **5l** over compound **5p**. Compound **5l** and **5p** exhibited MIC<sub>90</sub> values of 1.56 and 2.45 μM, respectively.

Altogether, the SAR analyses revealed that, in steric terms, the smaller cyclic amines **5a–5c** were as active as the larger aryl-piperazines **5d–5q**. Nevertheless, differences could be observed between the two sub-series. For instance, the compounds containing electron-withdrawing groups attached to the C-ring, such as halogens, appeared to have enhanced anti-*M.tb* activity compared to the compound without any substituents on the C ring (**5d**). Similarly, the compounds **5l** and **5q** containing other electron-withdrawing groups, such as acyl groups, were also potent in the anti-*M.tb* assay. However, no such relationship occurred in the electron-donating groups attached to the C-ring, such as in compounds **5e** and **5f**, which contained a methyl group and a methoxy group attached at the *para* position of the C ring, respectively. These compounds were not as potent as compound **5j** with an amine at the same position. Unlike compounds **5e** and **5f**, compound **5j** could act as a hydrogen-bond donor, which explains the difference in the activity between this compound and the ones with electron-donating groups. Among the compounds containing hetero-aromatic rings, the only compound demonstrating potency was compound **5n**, which contained 2-pyridyl as the C ring.

It is noteworthy that the most promising compounds in the series exhibited anti-TB activity profiles superior to several clinically used drugs that were included as positive controls in the present study. For instance, the most active compound **5n** (MIC<sub>90</sub> = 0.09 μM) exhibited activity higher than that of INH (MIC<sub>90</sub> = 0.95 μM) and LZD (MIC<sub>90</sub> = 0.74 μM) and statistically similar to that of RIF (MIC<sub>90</sub> = 0.05 μM). INH, LZD, and RIF are the drugs used widely in the treatment of susceptible and resistant forms of TB.

The cytotoxicity was evaluated on the MRC-5 cell line, as described previously<sup>[55,56]</sup> and the results were expressed as IC<sub>50</sub> values. This cell line is derived from healthy human lung

fibroblast tissue and is used widely for phenotypic screening in antituberculosis drug discovery.<sup>[57–59]</sup> The selectivity index (SI) of the evaluated compounds was the ratio between their IC<sub>50</sub> and MIC<sub>90</sub> values. All the Bfx derivatives in the first series exhibited a low cytotoxic profile against the MRC-5 cell line. The IC<sub>50</sub> values of all the final compounds were above 128 μM, reflecting high SI values for the most potent compounds (Table 1).

After the initial *in-vitro* biological evaluation, the lipophilic efficiency (LiPE) values for the compounds were determined (Table 1). Lipophilic efficiency is calculated from the biological activity data (anti-*M.tb* activity) and logD values and is used for selecting the most promising drug candidate compounds within a series. LiPE establishes a relationship between potency and lipophilia to estimate the differences among the compounds, considering not only the potency but also the physicochemical properties of the compounds. The literature recommends selecting the compounds with the highest LiPE values within a series to advance the discovery process.<sup>[60]</sup> In the present study, LiPE was calculated by subtracting the logD of the molecule from the negative log<sub>10</sub> of the potency (*M*) against the desired target. The logD values were calculated using ChemAxon's Calculator and the MIC<sub>90</sub> values were used as potency in the calculation of LiPE. It is noteworthy that the LiPE values presented here are only approximate LiPE values as the logD values used were calculated theoretically and not measured experimentally.

The LiPE values revealed the most promising compounds within the series worthy of being prioritized for further development. Compound **5n** emerged as the most promising one within the series, exhibiting not only a potent anti-*M.tb* activity but the highest LiPE value as well. Therefore, compound **5n** was used in the further molecular modification steps conducted to understand better the contribution of the other subunits of the molecule to its anti-*M.tb* activity.

The second series of compounds was designed based on the identification of the leading compound **5n** as the most promising one in the first series. The designing process involved the isosteric replacement of the Bfx ring with other aromatic and heteroaromatic rings to verify the importance that the benzofuroxanyl subunit has for the compound's anti-*M.tb*



activity. Furthermore, compound **11f** was designed by replacing the fluorine atom attached to the phenyl ring with a hydrogen atom to verify the contribution of the fluorine atom to the compound's biological activity.

The compounds **11a–11f** obtained in the second series were evaluated against *M.tb* H<sub>37</sub>Rv ATCC 27294. The compounds in which the Bfx subunit was replaced with another heterocycle exhibited a significant loss in the anti-*M.tb* activity. The MIC<sub>90</sub> values for these compounds (**11a–11e**) were above 25  $\mu$ M. These data indicated that the *N*-oxide-containing subunit present in the benzofuroxan is essential for biological activity. This fact was confirmed when compound **5n** was compared with its analog containing the benzofurazan ring (**11a**). The difference between the structures of these two compounds was the *N*-oxide subunit, which was present in the Bfx **5n** and absent in the benzofurazan **11a**. The simple removal of this subunit led to a complete loss of the anti-*M.tb* activity. These results suggested that the *N*-oxide subunit could be serving as a pharmacophoric group and the essential warhead. Previous studies have also demonstrated that Bfx derivatives interact with the thiol groups (–SH) present in the cysteine residues, often leading to enzymatic inhibition.<sup>[61,62]</sup> Therefore, we hypothesized that the Bfx nucleus could lead to the formation of a nitrous intermediate after biotransformation, which then served as an electrophilic site that would lead to the formation of an adduct after interaction with the cysteine residues (–SH) acting as nucleophiles.

The analog without the fluorine, compound **11f**, was quite potent despite the reduction in the anti-*M.tb* activity in relation to its parent compound **5n**. The MIC<sub>90</sub> value for compound **11f** was 2.5  $\mu$ M, accounting for a 27-fold reduction in the activity relative to the parent compound. The difference between these two compounds was the fluorine atom attached to the phenyl ring, present in compound **5n** and absent in compound **11f**. The latter contained a hydrogen atom at the same position. This result indicated that the fluorine atom, although not essential, has a certain contribution to the anti-*M.tb* activity.

## Further *in-vitro* biological profiling of selected compounds

The promising compounds in the first series selected for further evaluation based on their MIC<sub>90</sub> and LiPE values were assayed against a panel of clinical isolates, including MDR-TB and XDR-TB.<sup>[63]</sup> These strains were phenotypically characterized and exhibited resistance to several anti-*M.tb* drugs. Specifically, each MDR strain exhibited resistance to the following drugs: MDR-1: INH, RIF, and amikacin (AMK), MDR-2: INH and RIF, MDR-3: INH and RIF, MDR-4: INH, RIF, and AMK, and MDR-5: INH, RIF, AMK, and MOX. The strains were classified as MDR or XDR based on the MIC<sub>90</sub> values of control drugs against them.<sup>[54]</sup>

The MIC<sub>90</sub> values of the selected compounds against these strains varied (Table 2). For instance, most of the compounds exhibited potent activity against the XDR-TB strains (MDR-5), among which compounds **5a**, **5b**, **5n**, **5o**, and **5p** should be highlighted as these presented MIC<sub>90</sub> values against the XDR-TB strains in the range of 0.27–1.68  $\mu$ M. These compounds also exhibited potent activity against the MDR-1, MDR-2, MDR-3, and MDR-4 strains, with MIC<sub>90</sub> values ranging from 0.21 to 9.40  $\mu$ M against all the strains, the MIC<sub>90</sub> values exhibited by compounds **5a**, **5b**, **5n**, **5o**, and **5p** were below 10  $\mu$ M, confirming their potency against the resistant strains.

Clinical isolates differed significantly from the standard strains of ATCC. The H<sub>37</sub>Rv strain, which is used as the reference strain in most studies related to drug discovery, has certain limitations, as evidenced by the genetic diversity observed in the studies that compared its genome with those of the clinical isolates.<sup>[64]</sup> Both *in vitro* and *in vivo*, the differences in the profile of pathogenicity and virulence are important factors and, therefore, it is recommended to use different strains for a study to ensure reliable results and accurate prediction of the effect of the compound in a population.<sup>[64–66]</sup>

In the present study, compounds **5b** (Lapdesf-20–5b) and **5n** (Lapdesf-20–5n) were identified as the most potent against the resistant strains and, therefore, the most promising. These compounds demonstrated potent activity against all the

**Table 2.** Anti-*M.tb* activity of the most active compounds against the clinically isolated MDR-TB strains (MIC<sub>90</sub>).

Compound	MIC <sub>90</sub> [ $\mu$ M] MDR-1	MDR-2	MDR-3	MDR-4	MDR-5
<b>5a</b>	4.98 $\pm$ 4.56	1.38 $\pm$ 0.84	1.95 $\pm$ 1.22	2.20 $\pm$ 0.67	0.92 $\pm$ 0.47
<b>5b</b>	0.28 $\pm$ 0.02	< 0.27	< 0.27	< 0.27	< 0.27
<b>5g</b>	0.75 $\pm$ 0.33	2.47 $\pm$ 2.31	52.96 $\pm$ 0.80	> 53.43	33.39 $\pm$ 24.64
<b>5h</b>	4.65 $\pm$ 4.23	< 0.20	13.88 $\pm$ 8.70	16.53 $\pm$ 11.63	6.26 $\pm$ 6.16
<b>5i</b>	10.98 $\pm$ 10.09	2.35 $\pm$ 2.25	36.22 $\pm$ 21.78	> 48.80	3.55 $\pm$ 3.32
<b>5j</b>	4.84 $\pm$ 4.28	1.45 $\pm$ 0.03	4.55 $\pm$ 2.57	13.33 $\pm$ 0.05	3.88 $\pm$ 2.78
<b>5l</b>	16.80 $\pm$ 6.48	6.77 $\pm$ 5.43	18.23 $\pm$ 8.56	48.69 $\pm$ 5.51	2.18 $\pm$ 2.15
<b>5n</b>	0.56 $\pm$ 0.47	1.84 $\pm$ 1.73	0.26 $\pm$ 0.05	2.24 $\pm$ 1.47	1.68 $\pm$ 1.32
<b>5o</b>	9.40 $\pm$ 9.09	< 0.22	0.93 $\pm$ 0.62	1.21 $\pm$ 0.61	1.92 $\pm$ 1.55
<b>5p</b>	6.90 $\pm$ 6.01	1.47 $\pm$ 0.06	0.90 $\pm$ 0.30	1.06 $\pm$ 0.40	0.41 $\pm$ 0.01
<b>11f</b>	1.68 $\pm$ 0.78	1.43 $\pm$ 0.22	0.44 $\pm$ 0.31	0.61 $\pm$ 0.17	8.67 $\pm$ 7.84
LZD	N.D.	0.95 $\pm$ 0.01	0.58 $\pm$ 0.02	0.41 $\pm$ 0.03	0.47 $\pm$ 0.32
RIF	> 30.38	> 30.38	> 30.38	> 30.38	> 30.38
INH	> 182.30	> 182.30	71.56 $\pm$ 24.71	> 182.30	> 182.30
MOX	3.37 $\pm$ 0.69	0.40 $\pm$ 0.04	2.48 $\pm$ 1.12	4.69 $\pm$ 4.17	41.60 $\pm$ 35.81
AMK	> 42.69	5.33 $\pm$ 0.95	0.24 $\pm$ 0.10	> 42.69	19.52 $\pm$ 12.55
BZ8	> 25.00	> 25.00	> 25.00	> 25.00	> 25.00

INH: isoniazid; RIF: rifampicin; LZD: linezolid; MOX: moxifloxacin; AMK: amikacin;  $\pm$ : standard deviation (SD), average of three independent assays.

evaluated strains. For instance, compounds **5b** and **5n** presented MIC<sub>90</sub> values of 0.27 and 1.68  $\mu$ M, respectively, against the MDR-5 strain that is resistant to INH, RIF, AMK, and MOX (as evidenced by its phenotypic characterization). These results suggested that both **5b** and **5n** act through some mechanism of action that is different from the one used by the reference drugs.

The MDR-2 strain appeared to be the most sensitive to this class of compounds as most of these compounds exhibited MIC<sub>90</sub> values below 2.0  $\mu$ M against this strain. On the contrary, the MDR-1 strain appeared to be the most resistant to this class of compounds as most of the compounds exhibited MIC<sub>90</sub> values above 4.65  $\mu$ M against this strain. Compounds **5g**, **5i**, and **5l** were the least potent within this series as these compounds exhibited MIC<sub>90</sub> values above 30  $\mu$ M against the panel of resistant strains. Compound **11f**, the fluorine-free analog of compound **5n**, presented results similar to those presented by its parent compound **5n**. For instance, compounds **5n** and **11f** presented MIC<sub>90</sub> values of 1.84 and 1.43  $\mu$ M, respectively, against the MDR-2 strain, and the MIC<sub>90</sub> values of 0.26 and 0.44  $\mu$ M, respectively, against the MDR-3 strain. Despite the similar activity of these two compounds, the compound containing the fluorine atom, **5n**, was more promising as the fluorine atom provided greater lipophilicity to the parental compound **5n** (clog $P$ : 2.6) compared to the compound without the fluorine atom **11f** (clog $P$ : 2.2). In the development of anti-TB drugs, lipophilicity is an important parameter for consideration. Studies have reported that the compounds with log $P$  values within a certain range are likely to exhibit higher activity.<sup>[67,68]</sup>

Overall, eight among the 11 evaluated compounds exhibited potent anti-*M.tb* activity against the evaluated MDR strains. Among these eight compounds, **5b** and **5n** are noteworthy. Compound **5b** was particularly remarkable as it exhibited MIC<sub>90</sub> values below 0.28  $\mu$ M against all the MDR-*M.tb* strains, suggesting that this compound might have a mechanism of action different from that of all the others.

Altogether, the drug development and BZ8 optimization process led to the identification of a novel class of Bfx derivatives exhibiting an anti-*M.tb* activity profile superior to that of the parent compound BZ8. For instance, compound **5n** exhibited anti-*M.tb* activity against all the evaluated MDR-*M.tb* strains, with MIC<sub>90</sub> values below 2.3  $\mu$ M, while BZ8 demonstrated poor activity against the MDR-*M.tb* strains (MIC<sub>90</sub> > 25  $\mu$ M). These results do not imply that BZ8 is disqualified as a promising compound for the TB treatment as BZ8 has already demonstrated outstanding effectiveness in several previous *in vivo* studies conducted on mice infected with *M.tb*.<sup>[31]</sup> Nonetheless, BZ8 requires optimization so that it exhibits better anti-*M.tb* activity against the resistant strains. The strategy used in the present study was to replace the *N*-acylhydrazone subunit (BZ8) with an amide and the 4-pyridine ring (BZ8) with different heterocycles and cyclic amines, producing a class of compounds that are active against the MDR strains. Most of the compounds identified in the present work were active against the panel of the MDR-*M.tb* strains evaluated. In addition, the most active compounds exhibited no cytotoxicity in the

preliminary assays. Finally, the most active compounds also had higher clog $P$  values compared to the parent compound (BZ8).

These promising results against MDR-*M.tb* strains highlight the identified Bfx derivatives as leading candidate compounds for the discovery of novel drugs for the treatment of resistant forms of TB.

## Conclusion

This study aimed to evaluate the chemical instability and potency against MDR-*M.tb* strains of a novel series of benzofuroxan derivatives designed from the lead compound BZ8 already identified in previous studies. The synthesized novel compounds were more potent than the parent compound BZ8, in general, against a panel of MDR-*M.tb* strains evaluated. Compounds **5b** (Lapdesf-20-5b) and **5n** (Lapdesf-20-5n) were particularly remarkable in this regard as these demonstrated potent activities against all the evaluated strains. Compound **5b** was particularly superior, with MIC<sub>90</sub> values below 0.28  $\mu$ M against all the evaluated MDR-*M.tb* strains, thus suggesting that this compound might have a mechanism of action different from that of the other compounds. The BZ8 optimization process led to the discovery of a novel class of benzofuroxan derivatives exhibiting excellent potency against MDR-*M.tb* strains. Further studies are required for determining the mechanism of action of this novel class of compounds and assessing their *in vivo* activities.

## Experimental Section

### Chemistry

The melting points (mp) were measured using an electrothermal melting point apparatus (SMP3; Bibby Stuart Scientific). The <sup>1</sup>H and <sup>13</sup>C NMR spectra for all the compounds were obtained using a Bruker Fourier with Dual probe <sup>13</sup>C/<sup>1</sup>H (300-MHz) NMR spectrometer and Bruker Avance III HD 600 <sup>13</sup>C/<sup>1</sup>H (600-MHz) NMR spectrometer, respectively, with deuterated chloroform (CDCl<sub>3</sub>) or dimethylsulfoxide ([D<sub>6</sub>]DMSO) as the solvent. The chemical shifts were expressed in parts per million (ppm) relative to tetramethylsilane. The signal multiplicities were reported as singlet (s), doublet (d), doublet of doublet (dd), doublet of doublet of doublets (ddd), triplet (t), and multiplet (m). The compounds were purified using a chromatography column containing silica gel (60 Å pore size, 35–75  $\mu$ m particle size) and methanol, ethyl acetate, dichloromethane, hexane, and petroleum ether as solvents at a flow rate of approximately 15 mL/min. The progress of reaction for all the compounds was monitored using thin-layer chromatography (TLC) performed on 2.0 by 6.0 cm<sup>2</sup> aluminum sheets precoated with a 0.25-mm-thick layer of silica gel 60 (HF-254; Merck) and observed under UV light (265 nm). All the compounds were analyzed using HPLC, and their purity was confirmed to be greater than 98.5%. The HPLC conditions were as follows: Shimadzu HPLC model CBM 20-A (Shimadzu®) equipped with UV-VIS detector (model SPD-20A), quaternary pumping system mobile phase (model LC-20AT), solvent degasser (model DGU-20As), and an Agilent® Eclipse XDB C-18 column (250 mm × 274.6 mm; 5  $\mu$ m). An isocratic flow [methanol/water (70:30)] was used in the HPLC and the required reagents and solvents were purchased from commercial suppliers. Compounds **4**,

6, and 9 were synthesized according to previously described methodologies.<sup>[50–52]</sup> The synthetic intermediates **2a–2q**, **3a–3q**, **3n**, and **13** were also synthesized as described previously.<sup>[47–49]</sup> The chemical characterization data for all the synthetic intermediates are provided in the Supplementary Material.

## Synthesis

### General procedure for the synthesis of compounds **5a–5q**

A solution of 6-carboxybenzo[c][1,2,5]oxadiazole 1-oxide **4** (100 mg, 0.55 mmol) was stirred into 10 mL of anhydrous acetonitrile under nitrogen, followed by the addition of CDI (90 mg, 0.55 mmol). The reaction mixture was stirred for 90 min at room temperature and then a solution of the corresponding amine derivative **3a–3q** (0.33 mmol, 0.6 equiv. of the carboxylic acid **4**) in anhydrous acetonitrile (1 mL) was added dropwise. The resultant mixture was stirred at room temperature for 48 h under nitrogen atmosphere, followed by the removal of the solvent under reduced pressure. The obtained crude was washed with ethyl acetate. The solid reaction product was purified using flash chromatography on silica (EtOAc/petroleum ether, 20:80 to 70:30), producing the final compounds **5a–5q** in variable yields as described below.

**6-((4-(Azepan-1-yl)-3-fluorophenyl)carbamoyl)benzo[c][1,2,5]oxadiazole 1-N-oxide (5a).** Orange solid; yield 33%; mp: 232–235 °C; <sup>1</sup>H NMR (600 MHz, [D<sub>6</sub>]DMSO): δ = 10.55 (s, 1H), 8.64 (s, 1H), 8.18 (dd, *J* = 9.4; 0.9 Hz, 1H), 7.99 (dd, *J* = 9.4; 1.3 Hz, 1H), 7.62 (dd, *J* = 16.1; 2.4 Hz, 1H), 7.38 (dd, *J* = 8.9; 1.9 Hz, 1H), 6.93 (dd, *J* = 10.2; 9.0 Hz, 1H), 3.32–3.30 (m, 4H), 1.78–1.74 (m, 4H), 1.57–1.54 (m, 4H); <sup>13</sup>C NMR (151 MHz, [D<sub>6</sub>]DMSO): δ = 163.2, 152.5 (d, *J*<sub>C-F</sub> = 239.9 Hz, 1C), 136.0 (d, *J*<sub>C-F</sub> = 8.1 Hz, 1C), 132.7, 131.9, 130.0 (d, *J*<sub>C-F</sub> = 10.3 Hz, 1C), 117.0, 117.0 (d, *J*<sub>C-F</sub> = 5.3 Hz, 1C), 116.6, 116.5, 116.0, 109.1 (d, *J*<sub>C-F</sub> = 26.7 Hz, 1C), 51.6, 28.4, 26.6; anal. calcd (%) for C<sub>19</sub>H<sub>19</sub>FN<sub>4</sub>O<sub>3</sub>: C 61.61, H 5.17, N 15.13; found: C 61.60, H 5.16, N 15.13.

**6-((3-Fluoro-4-thiomorpholinophenyl)carbamoyl)benzo[c][1,2,5]oxadiazole 1-N-oxide (5b).** Pale yellow solid; yield 13%; mp: 242–245 °C; <sup>1</sup>H NMR (600 MHz, [D<sub>6</sub>]DMSO): δ = 10.57 (s, 1H), 8.28 (s, 1H), 8.00–7.73 (m, *J* = 37.4 Hz, 2H), 7.68 (d, *J* = 14.2 Hz, 1H), 7.45 (d, *J* = 8.3 Hz, 1H), 7.09 (t, *J* = 9.1 Hz, 1H), 3.22 (s, 4H), 2.75 (s, 4H); <sup>13</sup>C NMR (151 MHz, [D<sub>6</sub>]DMSO): δ = 162.8, 155.2 (d, *J*<sub>C-F</sub> = 243.2 Hz, 1C), 137.0 (d, *J*<sub>C-F</sub> = 8.7 Hz, 1C), 135.0, 133.9 (d, *J*<sub>C-F</sub> = 10.7 Hz, 1C), 132.8, 132.4, 132.0, 124.8, 120.4 (d, *J*<sub>C-F</sub> = 3.1 Hz, 1C), 116.4 (d, *J*<sub>C-F</sub> = 1.8 Hz, 1C), 108.5 (d, *J*<sub>C-F</sub> = 25.6 Hz, 1C), 53.0, 27.2; anal. calcd (%) for C<sub>17</sub>H<sub>15</sub>FN<sub>4</sub>O<sub>3</sub>S: C 54.54, H 4.04, N 14.97; found: C 54.56, H 4.05, N 14.97.

**6-((3-Fluoro-4-morpholinophenyl)carbamoyl)benzo[c][1,2,5]oxadiazole 1-N-oxide (5c).** Orange solid; yield 40%; mp: 192–193 °C; <sup>1</sup>H NMR (600 MHz, [D<sub>6</sub>]DMSO): δ = 10.57 (s, 1H), 8.46–8.20 (m, *J* = 25.6 Hz, 1H), 8.01–7.72 (m, *J* = 9.7 Hz, 2H), 7.68 (dd, *J* = 14.9, 2.2 Hz, 1H), 7.47 (dd, *J* = 8.7, 1.6 Hz, 1H), 7.06 (t, *J* = 9.3 Hz, 1H), 3.76–3.72 (m, 4H), 3.00–2.96 (m, 4H); <sup>13</sup>C NMR (151 MHz, [D<sub>6</sub>]DMSO): δ = 162.8, 155.0 (d, *J*<sub>C-F</sub> = 243.2 Hz, 1C), 136.0 (d, *J*<sub>C-F</sub> = 8.7 Hz, 1C), 134.9, 133.5 (d, *J*<sub>C-F</sub> = 10.5 Hz, 1C), 132.8, 132.3, 132.0, 124.8, 119.0 (d, *J*<sub>C-F</sub> = 3.8 Hz, 1C), 116.4 (d, *J*<sub>C-F</sub> = 2.3 Hz, 1C), 108.5 (d, *J*<sub>C-F</sub> = 25.6 Hz, 1C), 66.1, 50.6; anal. calcd (%) for C<sub>17</sub>H<sub>15</sub>FN<sub>4</sub>O<sub>4</sub>: C 56.98, H 4.22, N 15.64; found: C 56.98, H 4.20, N 15.63.

**6-((3-Fluoro-4-(4-phenylpiperazin-1-yl)phenyl)carbamoyl)benzo[c][1,2,5]oxadiazole 1-N-oxide (5d).** Yellow solid; yield 67%; mp: 203–204 °C; <sup>1</sup>H NMR (600 MHz, [D<sub>6</sub>]DMSO): δ = 10.60 (s, 1H), 7.71 (dd, *J* = 14.8, 2.3 Hz, 1H), 7.49 (dd, *J* = 8.7, 1.8 Hz, 1H), 7.24 (dd, *J* = 8.6, 7.4 Hz, 2H), 7.12 (t, *J* = 9.3 Hz, 1H), 7.00 (d, *J* = 8.0 Hz, 2H), 6.81 (t, *J* = 7.2 Hz, 1H), 3.29 (d, *J* = 9.8 Hz, 4H), 3.14 (d, *J* = 9.7 Hz, 4H); <sup>13</sup>C NMR (151 MHz, [D<sub>6</sub>]DMSO): δ = 162.7, 155.1 (d, *J*<sub>C-F</sub> = 243.0 Hz, 1C),

150.9, 136.0 (d, *J*<sub>C-F</sub> = 8.9 Hz, 1C), 134.6 (d, *J*<sub>C-F</sub> = 10.5 Hz, 1C), 133.5, 132.8, 132.3, 132.0, 129.0, 119.3 (d, *J*<sub>C-F</sub> = 24.9 Hz, 1C), 119.1, 116.5 (d, *J*<sub>C-F</sub> = 2.5 Hz, 1C), 115.6, 113.5, 108.6 (d, *J*<sub>C-F</sub> = 25.6 Hz, 1C), 50.3, 48.4; anal. calcd (%) for C<sub>23</sub>H<sub>20</sub>FN<sub>5</sub>O<sub>3</sub>: C 63.73, H 4.65, N 16.16; found: C 63.71, H 4.65, N 16.17.

**6-((3-Fluoro-4-(4-(*p*-tolyl)piperazin-1-yl)phenyl)carbamoyl)benzo[c][1,2,5]oxadiazole 1-N-oxide (5e).** Yellow solid; yield 65%; mp: 206–207 °C; <sup>1</sup>H NMR (600 MHz, [D<sub>6</sub>]DMSO): δ = 10.60 (s, 1H), 8.44–8.23 (m, *J* = 8.4 Hz, 1H), 8.04–7.74 (m, *J* = 8.4 Hz, 2H), 7.71 (dd, *J* = 14.8, 2.3 Hz, 1H), 7.48 (dd, *J* = 8.7, 1.6 Hz, 1H), 7.12 (t, *J* = 9.3 Hz, 1H), 7.05 (d, *J* = 8.2 Hz, 2H), 6.90 (d, *J* = 8.5 Hz, 2H), 3.24–3.21 (m, *J* = 4.2 Hz, 4H), 3.15–3.12 (m, *J* = 4.9 Hz, 4H), 2.21 (s, 3H); <sup>13</sup>C NMR (151 MHz, [D<sub>6</sub>]DMSO): δ = 162.9, 155.1 (d, *J*<sub>C-F</sub> = 243.0 Hz, 1C), 148.9, 136.1 (d, *J*<sub>C-F</sub> = 8.9 Hz, 1C), 134.6 (d, *J*<sub>C-F</sub> = 10.6 Hz, 1C), 133.6, 133.5, 132.8, 132.0, 129.4, 127.9, 119.3 (d, *J*<sub>C-F</sub> = 24.9 Hz, 1C), 116.5 (d, *J*<sub>C-F</sub> = 2.0 Hz, 1C), 115.9, 108.6 (d, *J*<sub>C-F</sub> = 25.8 Hz, 1C), 50.3, 48.9, 20.0; anal. calcd (%) for C<sub>24</sub>H<sub>22</sub>FN<sub>5</sub>O<sub>3</sub>: C 64.42, H 4.96, N 15.65; found: C 64.45, H 4.98, N 15.66.

**6-((3-Fluoro-4-(4-(4-methoxyphenyl)piperazin-1-yl)phenyl)carbamoyl)benzo[c][1,2,5]oxadiazole 1-N-oxide (5f).** Yellow solid; yield 55%; mp: 190–191 °C; <sup>1</sup>H NMR (600 MHz, [D<sub>6</sub>]DMSO): δ = 10.57 (s, 1H), 8.44–8.21 (m, *J* = 32.5 Hz, 1H), 8.03–7.73 (m, *J* = 9.5 Hz, 1H), 7.70 (dd, *J* = 14.8, 2.2 Hz, 1H), 7.48 (dd, *J* = 8.7, 1.5 Hz, 1H), 7.11 (t, *J* = 9.3 Hz, 1H), 6.95 (d, *J* = 9.1 Hz, 1H), 6.84 (d, *J* = 9.1 Hz, 1H), 3.69 (s, 1H), 3.16 (d, *J* = 5.5 Hz, 2H), 3.14 (d, *J* = 5.3 Hz, 2H); <sup>13</sup>C NMR (151 MHz, [D<sub>6</sub>]DMSO): δ = 162.7, 155.0 (d, *J*<sub>C-F</sub> = 243.3 Hz, 1C), 153.1, 145.3, 136.1 (d, *J*<sub>C-F</sub> = 8.9 Hz, 1C), 134.6 (d, *J*<sub>C-F</sub> = 10.7 Hz, 1C), 133.5, 132.8, 132.4, 132.0, 119.2 (d, *J*<sub>C-F</sub> = 24.9 Hz, 1C), 117.6, 116.4 (d, *J*<sub>C-F</sub> = 2.2 Hz, 1C), 114.2, 108.6 (d, *J*<sub>C-F</sub> = 25.8 Hz, 1C), 55.1, 50.3, 49.8; anal. calcd (%) for C<sub>24</sub>H<sub>22</sub>FN<sub>5</sub>O<sub>4</sub>: C 62.20, H 4.78, N 15.11; found: C 62.23, H 4.79, N 15.11.

**6-((3-Fluoro-4-(4-(4-fluorophenyl)piperazin-1-yl)phenyl)carbamoyl)benzo[c][1,2,5]oxadiazole 1-N-oxide (5g).** Pale brown solid; yield 37%; mp: 190–191 °C; <sup>1</sup>H NMR (600 MHz, [D<sub>6</sub>]DMSO): δ = 10.59 (s, 1H), 8.46–8.22 (m, 1H), 8.04–7.74 (m, 2H), 7.49 (dd, *J* = 8.7; 1.6 Hz, 1H), 7.71 (dd, *J* = 14.8; 2.2 Hz, 1H), 7.12 (t, *J* = 9.3 Hz, 1H), 7.09–7.05 (m, 2H), 7.03–7.00 (m, 2H), 3.25–3.22 (m, 4H), 3.16–3.13 (m, 4H); <sup>13</sup>C NMR (151 MHz, [D<sub>6</sub>]DMSO): δ = 162.9, 157.0 (d, *J*<sub>C-F</sub> = 235.8 Hz, 1C), 155.4 (d, *J*<sub>C-F</sub> = 243.0 Hz, 1C), 147.8 (d, *J*<sub>C-F</sub> = 4.1 Hz, 1C), 136.4 (d, *J*<sub>C-F</sub> = 8.9 Hz, 1C), 133.6 (d, *J*<sub>C-F</sub> = 10.5 Hz, 1C), 133.3, 133.0, 132.8, 132.6, 132.0, 119.3, 117.4 (d, *J*<sub>C-F</sub> = 7.4 Hz, 1C), 116.5 (d, *J*<sub>C-F</sub> = 1.9 Hz, 1C), 116.4, 115.4 (d, *J*<sub>C-F</sub> = 21.7 Hz, 1C), 108.6 (d, *J*<sub>C-F</sub> = 25.7 Hz, 1C), 50.3, 49.2; anal. calcd (%) for C<sub>23</sub>H<sub>19</sub>F<sub>2</sub>N<sub>5</sub>O<sub>3</sub>: C 61.19, H 4.24, N 15.51; found: C 61.21, H 4.25, N 15.50.

**6-((4-(4-(4-Chlorophenyl)piperazin-1-yl)-3-fluorophenyl)carbamoyl)benzo[c][1,2,5]oxadiazole 1-N-oxide (5h).** Off-white solid; yield 10%; mp: 202–205 °C; <sup>1</sup>H NMR (600 MHz, [D<sub>6</sub>]DMSO): δ = 10.60 (s, 1H), 8.46–8.23 (m, 1H), 8.03–7.76 (m, 2H), 7.71 (dd, *J* = 14.8; 2.3 Hz, 1H), 7.48 (dd, *J* = 8.7; 1.8 Hz, 1H), 7.26 (d, *J* = 9.0 Hz, 2H), 7.12 (t, *J* = 9.3 Hz, 1H), 7.01 (d, *J* = 9.1 Hz, 2H), 3.30–3.28 (m, 4H), 3.15–3.12 (m, 4H); <sup>13</sup>C NMR (151 MHz, [D<sub>6</sub>]DMSO): δ = 162.9, 155.1 (d, *J*<sub>C-F</sub> = 243.2 Hz, 1C), 149.7, 135.9 (d, *J*<sub>C-F</sub> = 8.9 Hz, 1C), 133.6 (d, *J*<sub>C-F</sub> = 10.6 Hz, 1C), 133.4, 133.0, 132.9 (d, *J*<sub>C-F</sub> = 12.0, 128.7, 128.6, 119.3 (d, *J*<sub>C-F</sub> = 3.9 Hz, 1C), 117.1, 116.5 (d, *J*<sub>C-F</sub> = 2.7 Hz, 1C), 116.4, 108.6 (d, *J*<sub>C-F</sub> = 25.6 Hz, 1C), 50.1, 48.2; anal. calcd (%) for C<sub>23</sub>H<sub>19</sub>ClFN<sub>5</sub>O<sub>3</sub>: C 59.04, H 4.09, N 14.97; found: C 59.02, H 4.07, N 14.97.

**6-((4-(4-(4-Bromophenyl)piperazin-1-yl)-3-fluorophenyl)carbamoyl)benzo[c][1,2,5]oxadiazole 1-N-oxide (5i).** Pale brown solid; yield 33%; mp: 199–203 °C; <sup>1</sup>H NMR (600 MHz, [D<sub>6</sub>]DMSO): δ = 10.60 (s, 1H), 8.45–8.22 (m, 1H), 8.03–7.74 (m, 2H), 7.71 (dd, *J* = 14.7; 2.1 Hz, 1H), 7.48 (d, *J* = 10.1 Hz, 1H), 7.37 (d, *J* = 8.9 Hz, 2H), 7.11 (t, *J* = 9.3 Hz, 1H), 6.96 (d, *J* = 9.0 Hz, 2H), 3.31–3.28 (m, 4H), 3.15–3.11 (m, 4H); <sup>13</sup>C NMR (151 MHz, [D<sub>6</sub>]DMSO): δ = 163.0, 155.1 (d, *J*<sub>C-F</sub> =

243.3 Hz, 1C), 150.1, 135.9 (d,  $J_{\text{C-F}} = 8.9$  Hz, 1C), 133.7, 133.6 (d,  $J_{\text{C-F}} = 10.7$  Hz, 1C), 132.8, 132.0, 131.6, 131.5, 119.3 (d,  $J_{\text{C-F}} = 3.8$  Hz, 1C), 117.5, 116.5 (d,  $J_{\text{C-F}} = 2.5$  Hz, 1C), 116.4, 110.3, 108.6 (d,  $J_{\text{C-F}} = 25.8$  Hz, 1C), 50.1, 48.1; anal. calcd (%) for  $\text{C}_{23}\text{H}_{19}\text{BrFN}_5\text{O}_3$ : C 53.92, H 3.74, N 13.67; found: C 53.95, H 3.76, N 13.69.

**6-((4-(4-(4-Aminophenyl)piperazin-1-yl)-3-fluorophenyl)carbamoyl)benzo[c][1,2,5]oxadiazole 1-N-oxide (5j).** Yellow solid; yield 97%; mp: 212–215 °C;  $^1\text{H}$  NMR (600 MHz,  $[\text{D}_6]\text{DMSO}$ ):  $\delta = 10.73$  (s, 1H), 8.48–8.27 (m, 1H), 8.05–7.80 (m, 2H), 7.73 (dd,  $J = 14.8$ ; 2.0 Hz, 1H), 7.52 (d,  $J = 8.6$  Hz, 1H), 7.10 (t,  $J = 9.3$  Hz, 1H), 6.75 (d,  $J = 8.7$  Hz, 2H), 6.51 (d,  $J = 8.7$  Hz, 2H), 4.61 (s, 1H), 3.11 (d,  $J = 4.9$  Hz, 4H), 3.06 (d,  $J = 4.5$  Hz, 4H);  $^{13}\text{C}$  NMR (151 MHz,  $[\text{D}_6]\text{DMSO}$ ):  $\delta = 162.4$ , 155.0 (d,  $J_{\text{C-F}} = 243.0$  Hz, 1C), 142.4, 139.0, 136.7 (d,  $J_{\text{C-F}} = 8.6$  Hz, 1C), 135.3, 134.2, 133.9 (d,  $J_{\text{C-F}} = 10.5$  Hz, 1C), 133.5, 133.1, 132.7, 118.2 (d,  $J_{\text{C-F}} = 3.8$  Hz, 1C), 116.5 (d,  $J_{\text{C-F}} = 2.7$  Hz, 1C), 114.7, 108.7 (d,  $J_{\text{C-F}} = 25.6$  Hz, 1C), 50.6, 50.5; anal. calcd (%) for  $\text{C}_{23}\text{H}_{21}\text{FN}_6\text{O}_3$ : C 61.60, H 4.72, N 18.74; found: C 61.65, H 4.74, N 18.75.

**6-((4-(4-(4-Ethoxycarbonyl)phenyl)piperazin-1-yl)-3-fluorophenyl)carbamoyl)benzo[c][1,2,5]oxadiazole 1-N-oxide (5k).** Orange solid; yield 54%; mp: 200–202 °C;  $^1\text{H}$  NMR (600 MHz,  $[\text{D}_6]\text{DMSO}$ ):  $\delta = 10.61$  (s, 1H), 8.42–8.24 (m, 1H), 8.08–7.87 (m, 2H), 7.81 (d,  $J = 8.7$  Hz, 2H), 7.72 (dd,  $J = 13.6$  Hz, 1H), 7.49 (dd,  $J = 8.6$  Hz, 1H), 7.12 (t,  $J = 9.3$  Hz, 1H), 7.05 (d,  $J = 8.7$  Hz, 2H), 4.24 (q,  $J = 7.0$  Hz, 2H), 3.51–3.45 (m, 4H), 3.15–3.12 (m, 4H), 1.29 (t,  $J = 7.1$  Hz, 3H);  $^{13}\text{C}$  NMR (151 MHz,  $[\text{D}_6]\text{DMSO}$ ):  $\delta = 165.6$ , 162.9, 153.8 (d,  $J_{\text{C-F}} = 243.3$  Hz, 1C), 135.9 (d,  $J_{\text{C-F}} = 8.5$  Hz, 1C), 135.8, 134.6, 133.7 (d,  $J_{\text{C-F}} = 10.5$  Hz, 1C), 133.3, 132.6, 131.4, 130.7, 119.4 (d,  $J_{\text{C-F}} = 4.0$  Hz, 1C), 118.7, 116.5 (d,  $J_{\text{C-F}} = 2.6$  Hz, 1C), 116.4, 113.6, 108.7 (d,  $J_{\text{C-F}} = 25.8$  Hz, 1C), 59.9, 50.0, 46.6, 14.3; anal. calcd (%) for  $\text{C}_{26}\text{H}_{24}\text{FN}_5\text{O}_5$ : C 61.78, H 4.79, N 13.85; found: C 61.75, H 4.78, N 13.86.

**6-((4-(4-(4-Acetylphenyl)piperazin-1-yl)-3-fluorophenyl)carbamoyl)benzo[c][1,2,5]oxadiazole 1-N-oxide (5l).** Pale brown solid; yield 27%; mp: 225–227 °C;  $^1\text{H}$  NMR (600 MHz,  $[\text{D}_6]\text{DMSO}$ ):  $\delta = 10.59$  (s, 1H), 8.44–8.23 (m, 1H), 8.04–7.86 (m, 2H), 7.83 (d,  $J = 8.8$  Hz, 2H), 7.72 (dd,  $J = 14.7$ ; 1.9 Hz, 1H), 7.49 (d,  $J = 8.5$  Hz, 1H), 7.12 (t,  $J = 9.3$  Hz, 1H), 7.04 (d,  $J = 8.9$  Hz, 2H), 3.52–3.48 (m, 4H), 3.15–3.12 (m, 4H), 2.46 (s, 3H);  $^{13}\text{C}$  NMR (151 MHz,  $[\text{D}_6]\text{DMSO}$ ):  $\delta = 195.7$ , 162.7, 155.1 (d,  $J_{\text{C-F}} = 243.5$  Hz, 1C), 135.9 (d,  $J_{\text{C-F}} = 8.9$  Hz, 1C), 135.8, 135.1, 134.6, 133.7 (d,  $J_{\text{C-F}} = 10.6$  Hz, 1C), 132.8, 132.0, 130.1, 119.4 (d,  $J_{\text{C-F}} = 3.7$  Hz, 1C), 116.5 (d,  $J_{\text{C-F}} = 2.6$  Hz, 1C), 116.4, 113.3, 108.6 (d,  $J_{\text{C-F}} = 25.5$  Hz, 1C), 50.0, 46.8, 26.1; anal. calcd (%) for  $\text{C}_{25}\text{H}_{22}\text{FN}_5\text{O}_4$ : C 63.15, H 4.66, N 14.73; found: C 63.15, H 4.65, N 14.75.

**6-((3-Fluoro-4-(4-(pyridin-4-yl)piperazin-1-yl)phenyl)carbamoyl)benzo[c][1,2,5]oxadiazole 1-N-oxide (5m).** Orange solid; yield 60%; mp: 222–225 °C;  $^1\text{H}$  NMR (600 MHz,  $[\text{D}_6]\text{DMSO}$ ):  $\delta = 10.65$  (s, 1H), 8.43–8.28 (m, 1H), 8.23 (t,  $J = 5.8$  Hz, 2H), 8.02–7.82 (m, 2H), 7.73 (d,  $J = 14.6$  Hz, 1H), 7.50 (d,  $J = 8.5$  Hz, 1H), 7.12 (t,  $J = 9.2$  Hz, 1H), 7.03 (d,  $J = 6.3$  Hz, 2H), 3.65–3.60 (m, 4H), 3.15–3.10 (m, 4H);  $^{13}\text{C}$  NMR (151 MHz,  $[\text{D}_6]\text{DMSO}$ ):  $\delta = 162.8$ , 155.3 (d,  $J_{\text{C-F}} = 243.2$  Hz, 1C), 153.5, 146.3, 135.6 (d,  $J_{\text{C-F}} = 8.7$  Hz, 1C), 133.9, 133.8 (d,  $J_{\text{C-F}} = 10.6$  Hz, 1C), 133.0, 132.0, 124.8, 119.5 (d,  $J_{\text{C-F}} = 3.9$  Hz, 1C), 116.5 (d,  $J_{\text{C-F}} = 3.0$  Hz, 1C), 116.4, 108.1 (d,  $J_{\text{C-F}} = 25.4$  Hz, 1C), 108.0, 49.8, 45.6; anal. calcd (%) for  $\text{C}_{22}\text{H}_{19}\text{FN}_6\text{O}_3$ : C 60.82, H 4.41, N 19.35; found: C 60.86, H 4.44, N 19.36.

**6-((3-Fluoro-4-(4-(pyridin-2-yl)piperazin-1-yl)phenyl)carbamoyl)benzo[c][1,2,5]oxadiazole 1-N-oxide (5n).** Orange solid; yield 50%; mp: 196–197 °C;  $^1\text{H}$  NMR (600 MHz,  $[\text{D}_6]\text{DMSO}$ ):  $\delta = 10.59$  (s, 1H), 8.41–8.22 (m, 1H), 8.14 (dd,  $J = 4.8$ ; 1.2 Hz, 1H), 8.02–7.75 (m, 2H), 7.71 (dd,  $J = 14.7$ ; 2.1 Hz, 1H), 7.59–7.53 (m, 1H), 7.48 (dd,  $J = 8.7$ ; 1.4 Hz, 1H), 7.11 (t,  $J = 9.3$  Hz, 1H), 6.89 (d,  $J = 8.6$  Hz, 1H), 6.67 (dd,  $J = 6.8$ ; 5.1 Hz, 1H), 3.66–3.62 (m, 4H), 3.11–3.07 (m, 4H);  $^{13}\text{C}$  NMR (151 MHz,  $[\text{D}_6]\text{DMSO}$ ):  $\delta = 162.6$ , 158.9, 155.1 (d,  $J_{\text{C-F}} = 243.1$  Hz, 1C),

147.6, 137.6, 136.1, 135.0 (d,  $J_{\text{C-F}} = 8.9$  Hz, 1C), 133.6 (d,  $J_{\text{C-F}} = 10.6$  Hz, 1C), 132.3, 132.0, 124.8, 119.4 (d,  $J_{\text{C-F}} = 3.8$  Hz, 1C), 116.4 (d,  $J_{\text{C-F}} = 2.6$  Hz, 1C), 113.2, 108.6 (d,  $J_{\text{C-F}} = 25.6$  Hz, 1C), 107.2, 50.1, 44.7; anal. calcd (%) for  $\text{C}_{22}\text{H}_{19}\text{FN}_6\text{O}_3$ : C 60.82, H 4.41, N 19.35; found: C 60.84, H 4.42, N 19.34.

**6-((3-Fluoro-4-(4-(pyrimidin-2-yl)piperazin-1-yl)phenyl)carbamoyl)benzo[c][1,2,5]oxadiazole 1-N-oxide (5o).** Pale brown solid; yield 58%; mp: 203–204 °C;  $^1\text{H}$  NMR (600 MHz,  $[\text{D}_6]\text{DMSO}$ ):  $\delta = 10.58$  (s, 1H), 8.39 (d,  $J = 4.7$  Hz, 2H), 8.36–8.21 (m, 1H), 8.02–7.75 (m, 2H), 7.71 (dd,  $J = 14.7$ ; 2.1 Hz, 1H), 7.47 (dd,  $J = 8.7$ ; 1.3 Hz, 1H), 7.10 (t,  $J = 9.3$  Hz, 1H), 6.66 (t,  $J = 4.7$  Hz, 1H), 3.91–3.87 (m, 4H), 3.07–3.03 (m, 4H);  $^{13}\text{C}$  NMR (151 MHz,  $[\text{D}_6]\text{DMSO}$ ):  $\delta = 162.7$ , 161.2, 158.0, 155.1 (d,  $J_{\text{C-F}} = 243.3$  Hz, 1C), 136.1 (d,  $J_{\text{C-F}} = 9.0$  Hz, 1C), 135.1, 133.7 (d,  $J_{\text{C-F}} = 10.6$  Hz, 1C), 132.8, 132.3, 132.0, 124.8, 119.5 (d,  $J_{\text{C-F}} = 3.5$  Hz, 1C), 116.4 (d,  $J_{\text{C-F}} = 2.5$  Hz, 1C), 108.6 (d,  $J_{\text{C-F}} = 25.5$  Hz, 1C), 108.4, 50.2, 43.3; anal. calcd (%) for  $\text{C}_{21}\text{H}_{18}\text{FN}_7\text{O}_3$ : C 57.93, H 4.17, N 22.52; found: C 57.91, H 4.15, N 22.51.

**6-((4-(4-Benzoylpiperazin-1-yl)-3-fluorophenyl)carbamoyl)benzo[c][1,2,5]oxadiazole 1-N-oxide (5p).** Yellow solid; yield 30%; mp: 238–240 °C;  $^1\text{H}$  NMR (600 MHz,  $[\text{D}_6]\text{DMSO}$ ):  $\delta = 10.59$  (s, 1H), 8.44–8.22 (m, 1H), 8.00–7.73 (m, 2H), 7.69 (dd,  $J = 14.6$ ; 2.2 Hz, 1H), 7.48–4.43 (m, 6H), 7.09 (t,  $J = 9.3$  Hz, 1H), 3.85–3.46 (m, 4H), 3.11–2.92 (m, 4H);  $^{13}\text{C}$  NMR (151 MHz,  $[\text{D}_6]\text{DMSO}$ ):  $\delta = 169.0$ , 162.2, 155.1 (d,  $J_{\text{C-F}} = 243.3$  Hz, 1C), 135.8 (d,  $J_{\text{C-F}} = 7.8$  Hz, 1C), 135.7, 134.8, 134.6, 133.9, 133.8 (d,  $J_{\text{C-F}} = 10.6$  Hz, 1C), 129.6, 128.5, 127.0, 119.7 (d,  $J_{\text{C-F}} = 3.5$  Hz, 1C), 116.4 (d,  $J_{\text{C-F}} = 2.6$  Hz, 1C), 108.6 (d,  $J_{\text{C-F}} = 25.6$  Hz, 1C), 50.6, 47.2; anal. calcd (%) for  $\text{C}_{24}\text{H}_{20}\text{FN}_5\text{O}_4$ : C 62.47, H 4.37, N 15.18; found: C 62.47, H 4.35, N 15.17.

**6-((4-(4-((tert-Butoxycarbonyl)amino)phenyl)piperazin-1-yl)-3-fluorophenyl)carbamoyl)benzo[c][1,2,5]oxadiazole 1-N-oxide (5q).** Off-white solid; yield 35%; mp: 195–199 °C;  $^1\text{H}$  NMR (600 MHz,  $[\text{D}_6]\text{DMSO}$ ):  $\delta = 10.58$  (s, 1H), 8.44–8.21 (m, 1H), 8.05–7.74 (m, 2H), 7.71 (dd,  $J = 14.8$ ; 2.2 Hz, 1H), 7.48 (dd,  $J = 8.7$ ; 1.5 Hz, 1H), 7.32 (d,  $J = 7.0$  Hz, 2H), 7.11 (t,  $J = 9.3$  Hz, 1H), 6.90 (d,  $J = 9.0$  Hz, 2H), 3.19 (d,  $J = 5.2$  Hz, 4H), 3.13 (d,  $J = 4.8$  Hz, 4H), 1.46 (s, 9H);  $^{13}\text{C}$  NMR (151 MHz,  $[\text{D}_6]\text{DMSO}$ ):  $\delta = 162.7$ , 155.0 (d,  $J_{\text{C-F}} = 243.0$  Hz, 1C), 153.4, 146.3, 136.0 (d,  $J_{\text{C-F}} = 8.6$  Hz, 1C), 134.6, 133.5 (d,  $J_{\text{C-F}} = 10.5$  Hz, 1C), 132.8, 132.0, 131.1, 119.3 (d,  $J_{\text{C-F}} = 3.6$  Hz, 1C), 119.2, 116.4 (d,  $J_{\text{C-F}} = 2.3$  Hz, 1C), 116.2, 108.6 (d,  $J_{\text{C-F}} = 25.5$  Hz, 1C), 78.5, 50.3, 49.2, 28.2; anal. calcd (%) for  $\text{C}_{28}\text{H}_{29}\text{FN}_6\text{O}_5$ : C 61.31, H 5.33, N 15.32; found: C 61.30, H 5.32, N 15.32.

### General procedure for the synthesis of compounds 11a–11f

A solution of the corresponding carboxylic acid **6**, **7**, **8**, **9**, or **10** (compound **6** = 100 mg, 0.61 mmol; compound **7** = 100 mg, 0.62 mmol; compound **8** = 100 mg, 0.61 mmol; compound **9** = 100 mg, 0.52 mmol; or compound **10** = 100 mg, 0.54 mmol) was stirred into 10 mL of anhydrous acetonitrile under nitrogen atmosphere, followed by the addition of CDI (1.0 equiv. of the corresponding carboxylic acid **6**, **7**, **8**, **9**, or **10**). The reaction mixture was stirred for 90 min at room temperature, after which a solution of the corresponding amine derivative **3n** (0.6 equiv. of the corresponding carboxylic acid **6**, **7**, **8**, **9**, or **10**) in anhydrous acetonitrile (1 mL) was added dropwise. The mixture was stirred at room temperature for 48 h under nitrogen, and then the solvent was removed under reduced pressure. The obtained crude was washed with ethyl acetate. The solid reaction product was purified using flash chromatography on silica (EtOAc/petroleum ether, 20:80 to 70:30), producing the final compounds **11a–11f** in variable yields as described below.

**N-(3-Fluoro-4-(4-(pyridin-2-yl)piperazin-1-yl)phenyl)benzo[c][1,2,5]oxadiazole-5-carboxamide (11a).** Yellow solid; yield 56%; mp: 244–247 °C;  $^1\text{H}$  NMR (600 MHz,  $[\text{D}_6]\text{DMSO}$ ):  $\delta = 12.03$  (s, 1H),



8.70 (s, 1H), 8.13 (ddd,  $J=4.9$ ; 1.9; 0.6 Hz, 1H), 7.64 (m, 1H), 7.55 (ddd,  $J=9.5$ ; 5.8; 2.2 Hz, 1H), 7.45 (dd,  $J=14.9$ ; 2.3 Hz, 1H), 7.06 (dd,  $J=8.7$ ; 2.2 Hz, 1H), 7.01 (t,  $J=9.2$  Hz, 1H), 6.88 (d,  $J=8.7$  Hz, 1H), 6.85 (d,  $J=8.6$ ; 0.7 Hz, 1H), 6.66 (dd,  $J=7.1$ ; 5.3 Hz, 1H), 3.64–3.61 (m, 4H), 3.05–3.01 (m, 4H);  $^{13}\text{C}$  NMR (151 MHz,  $[\text{D}_6]\text{DMSO}$ ):  $\delta=162.4$ , 159.0, 155.7, 154.1 (d,  $J_{\text{C-F}}=242.7$  Hz, 1C), 152.4, 147.6, 137.6, 135.1 (d,  $J_{\text{C-F}}=10.9$  Hz, 1C), 134.2 (d,  $J_{\text{C-F}}=9.3$  Hz, 1C), 124.1, 120.7, 119.7 (d,  $J_{\text{C-F}}=4.0$  Hz, 1C), 114.2 (d,  $J_{\text{C-F}}=2.7$  Hz, 1C), 113.2, 109.5, 107.2, 107.1, 106.7 (d,  $J_{\text{C-F}}=25.6$  Hz, 1C), 50.4, 44.8; anal. calcd (%) for  $\text{C}_{22}\text{H}_{19}\text{FN}_6\text{O}_2$ : C 63.15, H 4.58, N 20.08; found: C 63.13, H 4.55, N 20.09.

***N*-(3-Fluoro-4-(4-(pyridin-2-yl)piperazin-1-yl)phenyl)-1*H*-indole-5-carboxamide (11b).** Off-white solid; yield 51%; mp: 211–215 °C;  $^1\text{H}$  NMR (600 MHz,  $[\text{D}_6]\text{DMSO}$ ):  $\delta=11.40$  (s, 1H), 10.16 (s, 1H), 8.25 (s, 1H), 8.14 (dd,  $J=4.8$ ; 1.9 Hz, 1H), 7.78 (dd,  $J=15.0$ ; 2.3 Hz, 1H), 7.72 (dd,  $J=8.5$ ; 1.6 Hz, 1H), 7.58–7.54 (m, 1H), 7.52 (dd,  $J=8.7$ ; 1.8 Hz, 1H), 7.48 (d,  $J=8.5$  Hz, 1H), 7.47–7.46 (m, 1H), 7.08 (t,  $J=9.4$  Hz, 1H), 6.89 (d,  $J=8.6$  Hz, 1H), 6.67 (dd,  $J=7.1$ ; 4.9 Hz, 1H), 6.59–6.58 (m, 1H), 3.66–3.63 (m, 4H), 3.09–3.06 (m, 4H);  $^{13}\text{C}$  NMR (151 MHz,  $[\text{D}_6]\text{DMSO}$ ):  $\delta=166.4$ , 159.0, 155.2 (d,  $J_{\text{C-F}}=242.5$  Hz, 1C), 147.6, 137.6, 135.2 (d,  $J_{\text{C-F}}=8.9$  Hz, 1C), 135.1 (d,  $J_{\text{C-F}}=10.7$  Hz, 1C), 127.0, 125.5, 120.9, 119.3 (d,  $J_{\text{C-F}}=3.9$  Hz, 1C), 116.0 (d,  $J_{\text{C-F}}=2.7$  Hz, 1C), 113.2, 111.1, 108.3 (d,  $J_{\text{C-F}}=25.5$  Hz, 1C), 107.2, 102.2, 50.3, 44.8; anal. calcd (%) for  $\text{C}_{24}\text{H}_{22}\text{FN}_5\text{O}$ : C 69.38, H 5.34, N 16.86; found: C 69.37, H 5.37, N 16.85.

***N*-(3-Fluoro-4-(4-(pyridin-2-yl)piperazin-1-yl)phenyl)-1*H*-benzo[d]imidazole-5-carboxamide (11c).** Off-white solid; yield 32%; mp: 202–205 °C;  $^1\text{H}$  NMR (600 MHz,  $[\text{D}_6]\text{DMSO}$ ):  $\delta=13.03$  (s, 1H), 10.38 (s, 1H), 8.38 (s, 1H), 8.14 (dd,  $J=4.9$ ; 1.2 Hz, 2H), 7.85 (dd,  $J=8.6$  Hz, 1H), 7.80 (d,  $J=15.0$  Hz, 1H), 7.68 (dd,  $J=8.4$  Hz, 1H), 7.58–7.54 (m, 2H), 7.08 (t,  $J=9.3$  Hz, 1H), 6.89 (d,  $J=8.6$  Hz, 1H), 6.67 (dd,  $J=6.7$ ; 5.0 Hz, 1H), 3.66–3.61 (m, 4H), 3.09–3.05 (m, 4H);  $^{13}\text{C}$  NMR (151 MHz,  $[\text{D}_6]\text{DMSO}$ ):  $\delta=165.8$ , 159.0, 155.2 (d,  $J_{\text{C-F}}=242.3$  Hz, 1C), 147.6, 143.8, 142.4, 135.7 (d,  $J_{\text{C-F}}=8.7$  Hz, 1C), 135.3 (d,  $J_{\text{C-F}}=10.5$  Hz, 1C), 128.7, 127.9, 122.4, 119.3 (d,  $J_{\text{C-F}}=3.9$  Hz, 1C), 116.3, 116.2, 116.1 (d,  $J_{\text{C-F}}=2.4$  Hz, 1C), 113.2, 108.8 (d,  $J_{\text{C-F}}=26.1$  Hz, 1C), 107.2, 50.3, 44.8; anal. calcd (%) for  $\text{C}_{23}\text{H}_{21}\text{FN}_6\text{O}$ : C 66.33, H 5.08, N 20.18; found: C 66.33, H 5.11, N 20.20.

***N*-(3-Fluoro-4-(4-(pyridin-2-yl)piperazin-1-yl)phenyl)-4-(1*H*-tetrazol-5-yl)benzamide (11d).** Off-white solid; yield 71%; mp: 220–224 °C;  $^1\text{H}$  NMR (600 MHz,  $[\text{D}_6]\text{DMSO}$ ):  $\delta=10.46$  (s, 1H), 8.19 (d,  $J=8.3$  Hz, 1H), 8.15 (d,  $J=8.6$  Hz, 1H), 8.14–8.13 (m, 1H), 7.75 (dd,  $J=14.8$ ; 2.3 Hz, 1H), 7.51 (ddd,  $J=8.8$ ; 7.2; 2.0 Hz, 1H), 7.51 (dd,  $J=8.7$ ; 1.7 Hz, 1H), 7.11 (t, 1H), 6.90 (d,  $J=8.6$  Hz, 1H), 6.67 (dd,  $J=6.9$ ; 5.2 Hz, 1H), 3.66–3.63 (m, 4H), 3.10–3.07 (m, 4H);  $^{13}\text{C}$  NMR (151 MHz,  $[\text{D}_6]\text{DMSO}$ ):  $\delta=164.5$ , 158.9, 155.1 (d,  $J_{\text{C-F}}=243.0$  Hz, 1C), 147.5, 137.7, 136.7, 135.3 (d,  $J_{\text{C-F}}=8.9$  Hz, 1C), 134.1 (d,  $J_{\text{C-F}}=10.6$  Hz, 1C), 128.7, 127.3, 126.9, 119.3 (d,  $J_{\text{C-F}}=3.8$  Hz, 1C), 116.4 (d,  $J_{\text{C-F}}=2.7$  Hz, 1C), 113.3, 108.6 (d,  $J_{\text{C-F}}=25.5$  Hz, 1C), 107.3, 50.2, 44.8; anal. calcd (%) for  $\text{C}_{23}\text{H}_{21}\text{FN}_8\text{O}$ : C 62.15, H 4.76, N 25.21; found: C 62.18, H 4.78, N 25.24.

**4-Amino-*N*-(3-fluoro-4-(4-(pyridin-2-yl)piperazin-1-yl)phenyl)-3-nitrobenzamide (11e).** Yellow solid; yield 20%; mp: 199–205 °C;  $^1\text{H}$  NMR (600 MHz,  $[\text{D}_6]\text{DMSO}$ ):  $\delta=10.23$  (s, 1H), 8.71 (s, 1H), 8.14 (s, 1H), 7.97 (d,  $J=8.4$  Hz, 1H), 7.87 (s, 2H), 7.56 (t,  $J=7.2$  Hz, 1H), 7.46 (d,  $J=8.3$  Hz, 1H), 7.09 (s, 1H), 7.07 (d,  $J=9.7$  Hz, 1H), 6.69–6.65 (m, 1H), 3.65–3.62 (m, 4H), 3.09–3.06 (m, 4H);  $^{13}\text{C}$  NMR (151 MHz,  $[\text{D}_6]\text{DMSO}$ ):  $\delta=163.3$ , 159.0, 155.2 (d,  $J_{\text{C-F}}=242.7$  Hz, 1C), 148.0, 147.6, 137.6, 135.5 (d,  $J_{\text{C-F}}=8.9$  Hz, 1C), 134.4 (d,  $J_{\text{C-F}}=10.8$  Hz, 1C), 134.3, 125.9, 121.1, 119.2 (d,  $J_{\text{C-F}}=3.5$  Hz, 1C), 119.0, 116.3 (d,  $J_{\text{C-F}}=2.5$  Hz, 1C), 113.2, 107.2 (d,  $J_{\text{C-F}}=25.5$  Hz, 1C), 50.2, 44.8; anal. calcd (%) for  $\text{C}_{22}\text{H}_{21}\text{FN}_6\text{O}_3$ : C 60.54, H 4.85, N 19.26; found: C 60.55, H 4.88, N 19.28.

**6-((4-(4-(Pyridin-2-yl)piperazin-1-yl)phenyl)carbamoyl)benzo[c][1,2,5]oxadiazole 1-oxide (11f).** Orange solid; yield 71%; mp: 227–229 °C;  $^1\text{H}$  NMR (600 MHz,  $[\text{D}_6]\text{DMSO}$ ):  $\delta=10.41$  (s, 1H), 8.48–8.22 (m, 1H), 8.14 (d,  $J=3.3$  Hz, 1H), 8.06–7.74 (m, 2H), 7.65 (d,  $J=8.7$  Hz, 2H), 7.56 (t,  $J=7.1$  Hz, 1H), 7.02 (d,  $J=8.7$  Hz, 2H), 6.90 (d,  $J=8.4$  Hz, 1H), 6.69–6.65 (m, 1H), 3.67–3.60 (m, 4H), 3.25–3.19 (m, 4H);  $^{13}\text{C}$  NMR (151 MHz,  $[\text{D}_6]\text{DMSO}$ ):  $\delta=164.2$ , 159.0, 147.8, 147.6, 137.6, 135.8, 132.5, 130.7, 130.6, 128.2, 127.8, 121.5, 115.9, 113.2, 107.3, 48.4, 44.6; anal. calcd (%) for  $\text{C}_{22}\text{H}_{20}\text{N}_6\text{O}_3$ : C 63.45, H 4.84, N 20.18; found: C 63.49, H 4.86, N 20.20.

## Determination of minimal inhibitory concentration (MIC<sub>90</sub>)

According to Palomino et al.<sup>[53]</sup> the resazurin microtiter assay (REMA) was developed to determine the minimum inhibitory concentration (MIC<sub>90</sub>) of the compounds against the standard ( $H_37\text{Rv}$  ATCC 27294) and clinical isolates of *M. tuberculosis*. Briefly, 10 mg/mL solution of the compound in DMSO was diluted in the Middlebrook 7H9 broth supplemented with OADC (oleic acid, albumin, dextrose, and catalase) and 0.5% glycerol, in a concentration range of 0.09 to 25  $\mu\text{g/mL}$  in a 96-well microplate. The bacterial inoculum was cultured for 14 days (for standard strain) or 20 days (for clinical strains) until the optical density of McFarland no. 1 standard was reached, which was then adjusted to 10<sup>5</sup> CFU/mL, following which the culture was added to the microplates and incubated at 37 °C and 5% CO<sub>2</sub> atmosphere for seven days. Subsequently, resazurin was added, and after 24–48 h, the fluorescence was measured at 530/590 nm. The assays were performed in triplicate, and MIC<sub>90</sub> was defined as the average of the lowest concentrations [of the compound] that could inhibit the mycobacterial growth by 90%. In order to determine the resistance profile, a critical concentration based on a MycoTB Plate readout was used,<sup>[54]</sup> with the MICs above this critical concentration indicating the resistance of the strains to the tested drug. The critical concentrations used for INH, RFP, MOX/GAT, and AMK were 3.6, 2.4, 5.0, and 6.8  $\mu\text{M}$ , respectively.

## Cytotoxicity assay

The cytotoxicity of the compounds was determined in a human pulmonary fibroblast cell line (MRC-5-ATCC CCL-171) using the microdilution method in a 96-well plate. The cells were cultured with the DMEM supplemented with 10% fetal bovine serum, gentamicin sulfate (50 mg/L), and amphotericin B (2 mg/L). Subsequently, a concentration of  $2.5 \times 10^5$  cell/mL was seeded in a microplate and incubated at 37 °C and 5% CO<sub>2</sub> atmosphere for 24 h. After the incubation, the compounds were applied in a concentration range of 0.39–100  $\mu\text{g/mL}$ . After incubation for another 24 h, resazurin was added and then fluorescence was measured at 530/590 nm in a Synergy H1 microplate reader (BioTek). The assays were performed in triplicate and IC<sub>50</sub> was defined as the lowest concentration [of the compound] that could inhibit 50% of the inoculum.<sup>[56]</sup>

## Author Contributions

The manuscript was written through contributions of all authors. All authors have given approval to the final version of the manuscript.

## Acknowledgements

This study was supported by Fundação de Amparo à Pesquisa do Estado de São Paulo (FAPESP grants 2016/09502-7; 2018/17739-2; 2018/11079-0; 2018/00163-0; 2018/21778-3; 2018/24783-8). This study was financed in part by the Coordenação de Aperfeiçoamento de Pessoal de Nível Superior–Brasil (CAPES)–Finance Code 001 and Conselho Nacional de Desenvolvimento Científico e Tecnológico (CNPq 404181/2019-8 and 429139/2018-7). J.L.S. is CNPq productivity fellows' level 2 (CNPq Ref. Process: 304731/2017-0) and F.R.P. is CNPq productivity fellows' level 1D (CNPq Ref. Process: 303603/2018-6). Programa de Apoio ao Desenvolvimento Científico da Faculdade de Ciências Farmacêuticas da UNESP (PADC-FCF UNESP).

## Conflict of Interest

The authors declare no conflict of interest.

**Keywords:** antitubercular agents · benzofuroxan · multidrug-resistant TB · N-oxide · tuberculosis

- [1] T. M. Daniel, *Respir. Med.* **2006**, *100*, 1862–1870.
- [2] I. Barberis, N. L. Bragazzi, L. Galluzzo, M. Martini, *J. Prev. Med. Hyg.* **2017**, *58*, E9–E12.
- [3] World Health Organization, *Global Tuberculosis Report 2020*, Geneva, **2020**.
- [4] World Health Organization, *Global Tuberculosis Report 2016*, Geneva, **2016**.
- [5] World Health Organization, *Global Tuberculosis Report 2017*, Geneva, **2017**.
- [6] World Health Organization, *Global Tuberculosis Report 2018*, Geneva, **2018**.
- [7] World Health Organization, *Global Tuberculosis Report 2014*, Geneva, **2014**.
- [8] A. Zumla, P. Nahid, S. T. Cole, *Nat. Rev. Drug Discovery* **2013**, *12*, 388–404.
- [9] M. Klopfer, R. M. Warren, C. Hayes, N. C. G. van Pittius, E. M. Streicher, B. Muller, F. A. Sirgel, M. Chabula-Nxiweni, E. Hoosain, G. Coetzee, P. D. van Helden, T. C. Victor, A. P. Trollip, *Emerging Infect. Dis.* **2013**, *19*, 449–455.
- [10] A. Slomski, *JAMA J. Am. Med. Assoc.* **2013**, *309*, 1097–1098.
- [11] S. K. Parida, R. Axelsson-Robertson, M. V. Rao, N. Singh, I. Master, A. Lutckii, S. Keshavjee, J. Andersson, A. Zumla, M. Maeurer, *J. Intern. Med.* **2015**, *277*, 388–405.
- [12] M. Maeurer, M. Schito, A. Zumla, *Lancet Respir. Med.* **2014**, *2*, 256–257.
- [13] Z. F. Udawadia, R. A. Amale, K. K. Ajbani, C. Rodrigues, *Clin. Infect. Dis.* **2012**, *54*, 579–581.
- [14] A. A. Velayati, M. R. Masjedi, P. Farnia, P. Tabarsi, J. Ghanavi, A. H. ZiaZarifi, S. E. Hoffner, *Chest* **2009**, *136*, 420–425.
- [15] S. Chetty, M. Ramesh, A. Singh-Pillay, M. E. S. Soliman, *Bioorg. Med. Chem. Lett.* **2017**, *27*, 370–386.
- [16] A. Zumla, J. Chakaya, R. Centis, L. D'Ambrosio, P. Mwaba, M. Bates, N. Kapata, T. Nyirenda, D. Chanda, S. Mfinanga, M. Hoelscher, M. Maeurer, G. B. Migliori, *Lancet Respir. Med.* **2015**, *3*, 220–234.
- [17] Z. Ma, C. Lienhardt, H. McIlleron, A. J. Nunn, X. Wang, *Lancet* **2010**, *375*, 2100–2109.
- [18] A. R. Frydenberg, S. M. Graham, *Trop. Med. Int. Health* **2009**, *14*, 1329–1337.
- [19] S. A. Tasduq, P. Kaiser, S. C. Sharma, R. K. Johri, *Hepatol. Res.* **2007**, *37*, 845–853.
- [20] M. Singh, P. Sasi, G. Rai, V. H. Gupta, D. Amarapurkar, P. P. Wangikar, *Med. Chem. Res.* **2011**, *20*, 1611–1615.
- [21] D. Yee, C. Valiquette, M. Pelletier, I. Parisien, I. Rocher, D. Menzies, *Am. J. Respir. Crit. Care Med.* **2003**, *167*, 1472–1477.
- [22] V. Sahasrabudhe, T. Zhu, A. Vaz, S. Tse, *J. Infect. Dis.* **2015**, *211*, S107–S114.
- [23] World Health Organization, *Global Tuberculosis Report 2013*, Geneva, **2013**.
- [24] Stop TB Partnership, *The Paradigm Shift 2016–2020: Global Plan to End TB*, Geneva, **2015**.
- [25] A. Koul, N. Dendouga, K. Vergauwen, B. Molenberghs, L. Vranckx, R. Willebrords, Z. Ristic, H. Lill, I. Dorange, J. Guillemont, D. Bald, K. Andries, *Nat. Chem. Biol.* **2007**, *3*, 323–324.
- [26] P. Nahid, S. R. Mase, G. B. Migliori, G. Sotgiu, G. H. Bothamley, J. L. Brozek, A. Cattamanchi, J. P. Cegielski, L. Chen, C. L. Daley, T. L. Dalton, R. Duarte, F. Fregonese, C. R. Horsburgh, F. A. Khan, F. Kheir, Z. Lan, A. Lardizabal, M. Lauzardo, J. M. Mangan, S. M. Marks, L. McKenna, D. Menzies, C. D. Mitnick, D. M. Nilsen, F. Parvez, C. A. Peloquin, A. Raftery, H. S. Schaaf, N. S. Shah, J. R. Starke, J. W. Wilson, J. M. Wortham, T. Chorbha, B. Seaworth, *Am. J. Respir. Crit. Care Med.* **2019**, *200*, e93–e142.
- [27] M. Matsumoto, H. Hashizume, T. Tomishige, M. Kawasaki, H. Tsubouchi, H. Sasaki, Y. Shimokawa, M. Komatsu, *PLoS Med.* **2006**, *3*, e466.
- [28] U. Manjunatha, H. I. Boshoff, C. E. Barry, *Commun. Integr. Biol.* **2009**, *2*, 215–218.
- [29] M. D. J. Libardo, H. I. Boshoff, C. E. Barry, *Curr. Opin. Pharmacol.* **2018**, *42*, 81–94.
- [30] P. Hernández, R. Rojas, R. H. Gilman, M. Sauvain, L. M. Lima, E. J. Barreiro, M. González, H. Cerecetto, *Eur. J. Med. Chem.* **2013**, *59*, 64–74.
- [31] G. F. S. Fernandes, P. C. Souza, E. Moreno-Viguri, M. Santivañez-Veliz, R. Paucar, S. Pérez-Silanes, K. Chegaev, S. Guglielmo, L. Lazzarato, R. Fruttero, C. M. Chin, P. B. Da Silva, M. Chorilli, M. C. Solcia, C. M. Ribeiro, C. S. P. Silva, L. B. Marino, P. L. Bosquesi, D. M. Hunt, L. P. S. de Carvalho, C. A. D. S. Costa, S. Cho, Y. Wang, S. G. Franzblau, F. R. Pavan, J. L. Santos, *J. Med. Chem.* **2017**, *60*, 8647–8660.
- [32] G. F. S. Fernandes, P. C. Souza, L. B. Marino, K. Chegaev, S. Guglielmo, L. Lazzarato, R. Fruttero, M. C. Chung, F. R. Pavan, J. L. Santos, *Eur. J. Med. Chem.* **2016**, *123*, 523–531.
- [33] T. R. F. de Melo, C. Kumkhaek, G. F. D. S. Fernandes, M. E. L. Pires, R. C. Chelucci, K. P. Barbieri, F. Coelho, T. S. de O. Capote, C. Lanaro, I. Z. Carlos, S. Marcondes, K. Chegaev, S. Guglielmo, R. Fruttero, M. C. Chung, F. F. Costa, G. P. Rodgers, J. L. Dos Santos, *Eur. J. Med. Chem.* **2018**, *154*, 341–353.
- [34] H. Cerecetto, W. Porcal, *Mini-Rev. Med. Chem.* **2005**, *5*, 57–71.
- [35] G. F. S. Fernandes, A. R. Pavan, J. L. Santos, *Curr. Pharm. Des.* **2018**, *24*, 1325–1340.
- [36] M. Boiani, L. Piacenza, P. Hernandez, L. Boiani, H. Cerecetto, M. Gonzalez, A. Denicola, *Biochem. Pharmacol.* **2010**, *79*, 1736–1745.
- [37] D. Castro, L. Boiani, D. Benitez, P. Hernandez, A. Merlino, C. Gil, C. Olea-Azar, M. Gonzalez, H. Cerecetto, W. Porcal, *Eur. J. Med. Chem.* **2009**, *44*, 5055–5065.
- [38] C. Olea-Azar, C. Rigol, F. Mendizábal, H. Cerecetto, R. Di Maio, M. González, W. Porcal, A. Morello, Y. Repetto, J. D. Maya, *Lett. Drug Des. Discovery* **2005**, *2*, 294–301.
- [39] S. D. Jorge, F. Palace-Berl, K. F. M. Pasqualoto, M. Ishii, A. K. Ferreira, C. M. Berra, R. V. Bosch, D. A. Maria, L. C. Tavares, *Eur. J. Med. Chem.* **2013**, *64*, 200–214.
- [40] O. Mestre, R. Hurtado-Ortiz, T. Dos Vultos, A. Namouchi, M. Cimino, M. Pimentel, O. Neyrolles, B. Gicquel, *PLoS One* **2013**, *8*, e53486.
- [41] M. I. Voskuil, I. L. Bartek, K. Visconti, G. K. Schoolnik, *Front. Microbiol.* **2011**, *2*, 1–12.
- [42] S. M. Behar, C. J. Martin, M. G. Booty, T. Nishimura, X. Zhao, H.-X. Gan, M. Divangahi, H. G. Remold, *Mucosal Immunol.* **2011**, *4*, 279–87.
- [43] N. Perskvist, M. Long, O. Stendahl, L. Zheng, *J. Immunol.* **2002**, *168*, 6358–6365.
- [44] J. Šarlauskas, V. Miliukienė, Ž. Anusevičius, L. Misevičienė, K. Krikštopaitis, A. Nemeikaitė-Čėnienė, I. Vitėnienė, N. Čėnas, *Chemija* **2009**, *20*, 109–115.
- [45] A. T. Dharmaraja, M. Alvala, D. Sriram, P. Yogeeswari, H. Chakrapani, *Chem. Commun.* **2012**, *48*, 10325–7.
- [46] F. C. Fang, *Nat. Rev. Microbiol.* **2004**, *2*, 820–832.
- [47] X. Boxuan, D. Xiudong, W. Yachuang, C. Le, Q. Ping, W. Di, Z. Yanfang, *Chem. Res. Chin. Univ.* **2018**, *34*, 51–56.
- [48] P. Xiang, T. Zhou, L. Wang, C.-Y. Sun, J. Hu, Y.-L. Zhao, L. Yang, *Molecules* **2012**, *17*, 873–883.
- [49] Q. Feng, W. Ying, *Drug for Preventing or Treating Mycobacterial Diseases*, WO2013182070 A1, **2013**.
- [50] P. B. Ghosh, M. W. Whitehouse, *J. Med. Chem.* **1968**, *11*, 305–311.



- [51] L. Keurulainen, M. Heiskari, S. Nenonen, A. Nasereddin, D. Kopelyanskiy, T. Leino, J. Yli-Kauhaluoma, C. Jaffe, P. Kiuru, *MedChemComm* **2015**, *6*, 1673–1678.
- [52] M. Koyama, N. Ohtani, F. Kai, I. Moriguchi, S. Inouye, *J. Med. Chem.* **1987**, *30*, 552–562.
- [53] J. Palomino, A. Martin, M. Camacho, H. Guerra, J. Swings, F. Portaels, *Antimicrob. Agents Chemother.* **2002**, *46*, 2720–2722.
- [54] S. K. Heysell, S. Pholwat, S. G. Mpagama, S. J. Pazia, H. Kumburu, N. Ndusilo, J. Gratz, E. R. Houpt, G. S. Kibiki, *Antimicrob. Agents Chemother.* **2015**, *59*, 7104–7108.
- [55] F. R. Pavan, P. I. D. S. Maia, S. R. a Leite, V. M. Defflon, A. a. Batista, D. N. Sato, S. G. Franzblau, C. Q. F. Leite, *Eur. J. Med. Chem.* **2010**, *45*, 1898–1905.
- [56] D. L. Campos, I. Machado, C. M. Ribeiro, D. Gambino, F. R. Pavan, *J. Antibiot. (Tokyo)*. **2020**, *73*, 120–124.
- [57] V. Straniero, M. Pallavicini, G. Chiodini, C. Zanotto, L. Volonte, A. Radaelli, C. Bolchi, L. Fumagalli, M. Sanguinetti, G. Menchinelli, G. Delogu, B. Battah, C. D. G. Morghen, E. Valoti, *Eur. J. Med. Chem.* **2016**, *120*, 227–243.
- [58] A. A. Wube, F. Bucar, C. Hochfellner, M. Blunder, R. Bauer, A. Hüfner, *Eur. J. Med. Chem.* **2011**, *46*, 2091–2101.
- [59] D. U. Ganihigama, S. Sureram, S. Sangher, P. Hongmanee, T. Aree, C. Mahidol, S. Ruchirawat, P. Kittakooop, *Eur. J. Med. Chem.* **2015**, *89*, 1–12.
- [60] T. W. Johnson, R. A. Gallego, M. P. Edwards, *J. Med. Chem.* **2018**, *61*, 6401–6420.
- [61] I. S. Severina, L. N. Axenova, A. V. Veselovsky, N. V. Pyatakova, O. A. Buneeva, A. S. Ivanov, A. E. Medvedev, *Biochem.* **2003**, *68*, 1048–1054.
- [62] A. Y. Kots, M. A. Grafov, Y. V. Khropov, V. L. Betin, N. N. Belushkina, O. G. Busygina, M. Y. Yazykova, I. V. Ovchinnikov, A. S. Kulikov, N. N. Makhova, N. A. Medvedeva, T. V. Bulargina, I. S. Severina, *Br. J. Pharmacol.* **2000**, *129*, 1163–1177.
- [63] M. Miyata, F. R. Pavan, D. N. Sato, L. B. Marino, M. H. Hirata, R. F. Cardoso, F. A. F. de Melo, C. F. Zanelli, C. Q. F. Leite, *Biomed. Pharmacother.* **2011**, *65*, 456–459.
- [64] R. F. O'Toole, S. S. Gautam, *Genomics* **2017**, *109*, 471–474.
- [65] A. G. Ramos-Martinez, M. A. Valtierra-Alvarado, M. H. Garcia-Hernandez, R. Hernandez-Pando, J. E. Castañeda-Delgado, C. Cougoule, B. Rivas-Santiago, O. Neyrolles, J. A. Enciso-Moreno, G. Lugo-Villarino, C. J. Serrano, *Mem. Inst. Oswaldo Cruz* **2019**, *114*, e190102.
- [66] T. Heunis, A. Dippenaar, R. M. Warren, P. D. van Helden, R. G. van der Merwe, N. C. G. van Pittius, A. Pain, S. L. Sampson, D. L. Tabb, *J. Proteome Res.* **2017**, *16*, 3841–3851.
- [67] G. F. S. Fernandes, D. H. Jornada, P. C. Souza, C. Man Chin, F. R. Pavan, J. L. Santos, *Curr. Med. Chem.* **2015**, *22*, 3133–3161.
- [68] G. F. dos S. Fernandes, C. M. Chin, J. L. Dos Santos, *Pharmaceuticals* **2017**, *10*, 51.

---

Manuscript received: November 18, 2020  
Revised manuscript received: January 6, 2021  
Accepted manuscript online: January 6, 2021  
Version of record online: February 9, 2021